October 2018 | EPA/600/R-18/365 | www.epa.gov/research

EPA
United States
Environmental Protection
Agency

Runoff and Sediment Yield on the US-Mexico Border, Los Laureles Canyon

EPA EXTERNAL REPORT

Office of Research and Development
National Exposure Research Laboratory

External Report
October 2018

Runoff and Sediment Yield on the US-Mexico Border, Los Laureles Canyon

Trent W. Biggs[1], Kris Taniguchi[1], Napoleon Gudiño-Elizondo[2], Eddy Langendoen[3], Yongping Yuan[4], Ron Bingner[3], Doug Liden[5]

[1] Department of Geography, San Diego State University, San Diego, CA
[2] Centro de Investigación Científica y de Educación Superior de Ensenada, Baja California, Mexico
[3] USDA-ARS-National Sedimentation Laboratory, Oxford, MS
[4] EPA- Office of Research and Development, Research Triangle Park, NC
[5] EPA-Region 9 San Diego Border Office, San Diego, CA

Preface

This document was created to introduce researches completed on the regional applied research effort (RARE) project "Sediment Load Estimation of the Tijuana River Watershed Under Existing Conditions and the Future Alternative Scenarios for Best Management Practice Implementation". Excessive flooding and sedimentation threaten both ecosystems and human populations. On the US-Mexico border, the Tijuana Estuary in the United States suffers from "excessive sedimentation", which requires expensive maintenance of sediment traps in the United States. Excessive sedimentation also damages infrastructure, particularly, in Mexico communities, which result in disruption of services and mortality. Thus, determining the source of the sediment and mitigating its production is a primary management goal of the US EPA and other cross-border agencies. Despite the importance of erosion and sedimentation for the well-being of humans and ecosystems on the US-Mexico border, little data exists to successfully measure and model the impact of urbanization on watershed processes. This study was intended to fill this gap by presenting an integrated dataset necessary for supporting comprehensive study of runoff, soil erosion and sediment production in this region.

Acknowledgements

We acknowledge the contributions of the other agencies including San Diego State University, the USDA-ARS, Dr. Thomas Kretzschmar, the Centro de Investigación Científica y de Educación Superior de Ensenada. Authors would like to thank Dr. Heather Golden, Chi-Hua Huang, Steve Kraemer, and Roger Kuhnle for reviewing the report and providing helpful feedback and suggestions. Thanks also go to Fernando Jagueri for help with sediment sampling, and to various residents of Los Laureles for housing and maintaining equipment.

Disclaimer

Contact Information

If you have questions or need additional information, email the project lead Yongping Yuan at yuan.yongping@epa.gov or professor Trent Biggs at tbiggs@sdsu.edu or go to the project website (https://biggslab.sdsu.edu/?page_id=50).

Executive Summary

The Tijuana River Watershed (TRW), which drains 4465 km^2, including 3,253 km^2 (73%) in Mexico and 1,212 km^2 (27%) in US, has experienced large losses of sediment from sheet and rill erosion, gully formation, and channel erosion. Excessive soil erosion and transport and deposition of sediment in the watershed have caused many detrimental effects to the people living in the watershed. Communities on both sides of the US-Mexico border are adversely affected by increased flooding from vegetation removal and paving, and communities in Mexico in particular experience disruption of services and transportation due to erosion of unpaved roads. Furthermore, sediment loading from the watershed also impairs conditions for ecosystems in the Tijuana estuary. This project seeks to address Region 9 Science Council priorities associated with Sec. 303 [33 USC 1313] and Sec. 319 [33 USC 1329] of the Clean Water Act (CWA) and the National Environmental Policy Act (NEPA). The long-term research objective of this project is to gain better understanding on how urbanization affects both ecosystems and human populations along the US-Mexico border. Realization of the detailed objective to achieve the long-term protection of ecosystems in the Tijuana estuary and human population includes field data collection and modeling and analysis of the critical factors impacting different erosion processes (sheet and rill, gully, channel). The results of this effort will be used to determine an effective approach for sediment loading estimation as well as evaluating the mitigation of sediment loads that could result from implementation of conservation easements, re-vegetation, sediment basins, paving, and other Best Management Practices (BMP).

The first report (Runoff and Sediment Yield on the US-Mexico Border, Los Laureles Canyon) presents an integrated dataset necessary for supporting comprehensive analysis and modeling of runoff, soil erosion and sediment production. In order to quantify erosion processes in detail, data collection focused on Los Laureles Canyon watershed (LLCW), one sub-watershed of the TRW draining to the Tijuana estuary. The dataset includes rainfall, runoff, suspended sediment concentration, and sediment yield observed in sediment traps. Secondly, this report describes the rainfall-runoff-sediment relationships in the watershed and how rainfall type and intensity affect those relationships. Finally, total sediment yields at the outlet from the LLCW were compared with other natural and urbanized watersheds in southern California. In this report, section 2.1 describes rainfall data. Section 2.2 describes runoff data, including depth sensors installed at the outlet, discharge calculation (section 2.2.2), and definition of events for hydrological analysis (Section 2.2.3). Section 2.3 describes suspended sediment concentrations and loads, Section 2.4 describes sediment observed in the sediment traps at the outlet and corrections for trap efficiency, and Section 2.5 describes sediment accumulation in a newly constructed sediment retention basin in Mexico. Together, the data provide a baseline of water and sediment load across the border. The central findings include: 1) the rainfall-runoff relationship can be approximated with an SCS CN of 80-90 which is consistent with the urban land cover; 2) 6-hour rainfall intensity was a key control on peak runoff production; 3) suspended sediment concentration was relatively stable at high discharge, with a volume weighted mean of ~20 g/L; 4) total annual sediment load observed at the outlet correlated linearly with annual rainfall, and 5) annual sediment load was ~5000 tons km^{-2} per year, which is ~10x higher than other urbanized watersheds in southern California and among the highest rates observed in the southwestern US.

Table of Contents

1. INTRODUCTION

1.1. Background Information and Objectives

Excessive flooding and sedimentation threaten both ecosystems and human populations. On the US-Mexico border, urbanization has increased runoff and sedimentation loads. In the Tijuana-San Diego region, the Tijuana Estuary in the United States suffers from "excessive sedimentation" (Weis et al, 2001), and determining the source of the sediment and mitigating its production is a primary management goal of the US EPA and other cross-border agencies.

Urbanization in Mexico differs from urbanization in the United States, with a longer duration of the phase of exposed soil (Biggs et al, 2010), where vacant lots and unpaved roads may have high sediment production for decades. Over a decadal time-scale, urbanized watersheds gradually accumulate impervious surfaces and earthen channels are lined with concrete, resulting in decreased sediment production but increased runoff and perhaps increased channel erosion downstream of paved watersheds and channelized reaches. Communities on both sides of the US-Mexico border are adversely affected by human-induced watershed alteration, including increased flooding from vegetation removal and paving, and communities in Mexico in particular experience disruption of services and transportation due to erosion of unpaved roads. A majority of residents in Los Laureles Canyon on the US-Mexico border report that they are impacted by flooding and/or road damage due to storms (Grover and Swanson, 2011).

Despite the importance of erosion, sediment loads and runoff for the well-being of humans and ecosystems on the US-Mexico border, little data exists to successfully measure and model the impact of urbanization on watershed processes. The objectives of this report are to:

1. Present an integrated dataset necessary for supporting comprehensive modeling of runoff, soil erosion and sediment production in a small watershed draining to the Tijuana estuary. The dataset includes rainfall, runoff, suspended sediment concentration, and sediment yield observed in sediment traps.

2. Describe the rainfall-runoff-sediment relationships in the watershed and how rainfall type and intensity affect those relationships.

3. Compare total sediment yield at the outlet with other natural and urbanized watersheds in southern California.

The study included collection of 5-minute rainfall and runoff for ten events (2014-2016), collection of water samples for measurement of suspended sediment concentration, compilation of data on annual sediment yield at a sediment trap in the United States (2006-2014) and analyses of sediment texture for traps in the US and Mexico.

1.2. Study Area

The Los Laureles Canyon watershed (LLCW) lies on the US-Mexico border (Figure 1.1). The climate is semi-arid Mediterranean, with a wet season from November to April and mean annual precipitation of ~100 mm/yr. The LLCW is on the San Diego Formation, which includes marine and fluvial sediment deposits that include conglomerate, sandy conglomerate, and siltstone. Soils include cobbly sandy loams and sandy loams, some of which are highly erodible when disturbed. Slopes are steepest on the incised canyons of the downstream sections of the mainstem. Mean slope as measured by a 5 m-resolution LiDAR digital elevation model from 2006 is 13.5º, with a maximum slope of 63º.

The watershed drains southeast to northwest. The outlet of the watershed for the purposes of this study is defined by the outlet of a pair of sediment traps in the United States. The drainage area at the outlet of the sediment trap is 11.57 km^2, with 0.59 km^2 in the United States and 10.98 km^2 in Mexico (Figure 1.1).

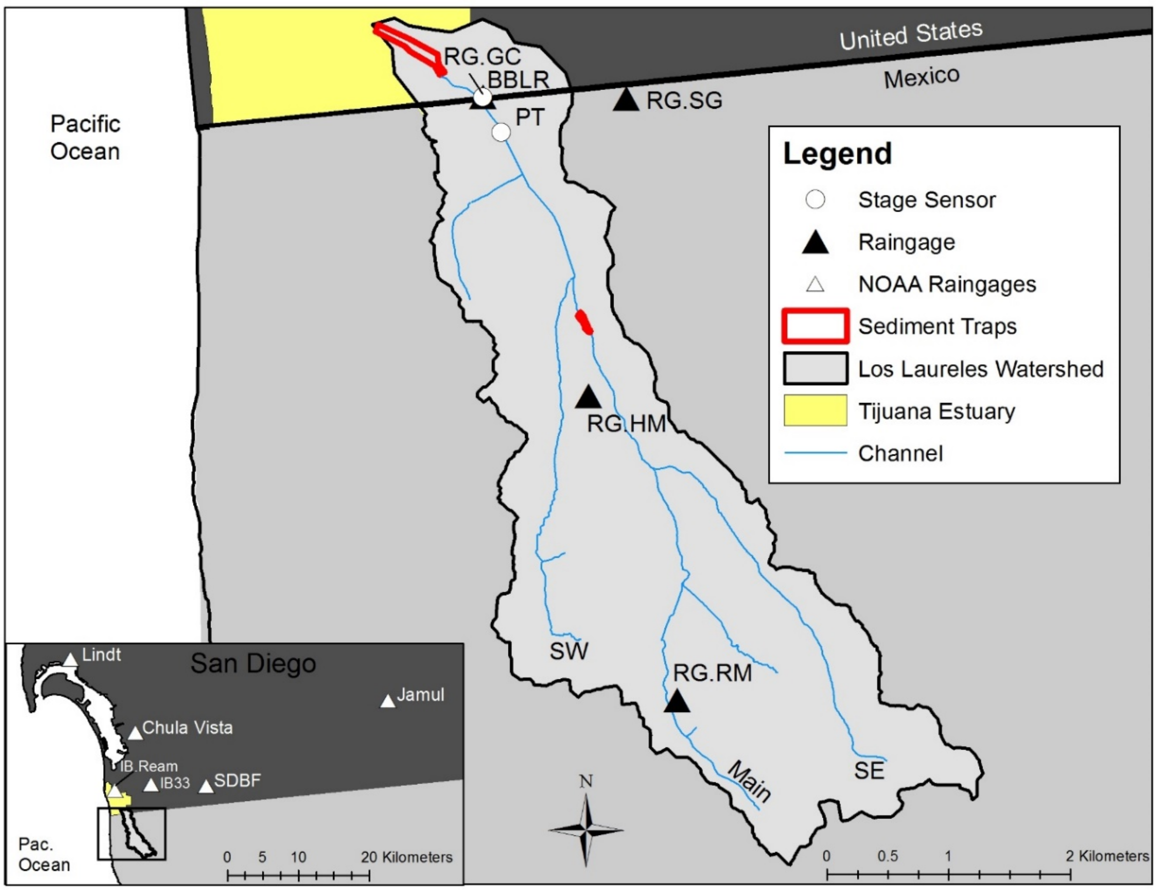

Figure 1.1. Rain gage (RG), pressure transducer (PT), field camera, and the US and Mexico sedimentation basin locations with Los Laureles Canyon watershed boundary. BBLR is the water depth bubbler maintained by the International Boundary Water Commission (IBWC). Three tributaries are labelled: Main, SW, and SE. The inset location map shows six rain gages near LLCW (white triangles) maintained by the National Oceanic and Atmospheric Administration (NOAA) or the International Boundary Water Commission (IBWC).

The watershed was urbanized starting in 1962, with most urbanization occurring between 1980 and 2002 (Figure 1.2). Much of the urbanized area is in "irregular" settlements that are not part of the formal planning process and are unregulated by the City of Tijuana or other central planning authority. The watershed is approximately 30% impervious, as calculated with maps from Biggs et al (2010) updated with visual interpretation of Google Earth™ imagery (K. Taniguchi, unpublished data).

In 2005, two sediment traps were constructed in the United States on the course of the main stream before it flows into the Tijuana Estuary (Figure 1.1). The traps have a combined capacity of approximately 185,804 to 234,830 tons of sediment (based on bulk density of 1.67 tons/m^3) and were designed to capture excessive sediment and prevent it from depositing in the estuary (SWIA, 2001). In 2015, an additional sediment trap was installed in Mexico, just downstream of the confluence of a major tributary (southeast channel) but upstream of another tributary (SW channel) (Figure 1.1).

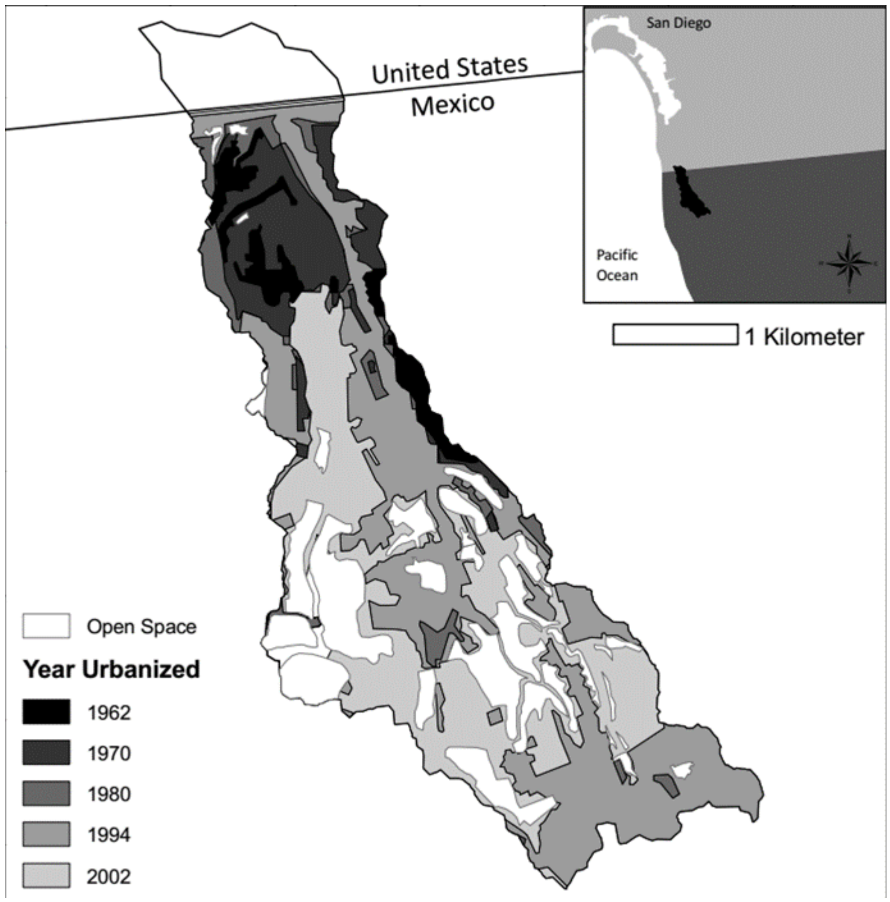

FIGURE 1.2. Map of the urban area by year urbanized (1962-2002) in the Los Laureles Canyon watershed. Data described in Biggs et al (2010).

2. METHODS AND RESULTS

2.1 Rainfall

2.1.1. Rain gages in and near the watershed, 2014-2017

Two rain gages in LLCW collected data for all events that occurred during the study period (2014-2016), one near the center of the watershed at Hormiguitas (RG.HM, Figure 1.1), and another at the mouth of the LLCW upstream of the US sediment traps (RG.GC, Figure 1.1). A third rain gage is in a neighboring watershed 1.2 km east of RG.GC at Smuggler's Gulch (RG.SG, Figure 1.1). A fourth rain gage was installed in the southeast channel, but was disturbed during subsequent construction at the installation site and did not record data. A fifth gage was installed at RG.RM in April 2016. A sixth rain gage installed near RG.RM in 2014 malfunctioned. Rainfall data were collected for all events at RG.HM and RG.GC and for all events except those between 1/25/2015 and 6/1/2015 at RG.SG; data for that period were lost during data transfer at the County meteorology office (R. Allen, personal communication, March 2016).

Rainfall at HM was higher than rainfall at GC by an average of 23% and by 17% for total rainfall, which is consistent with a small orographic effect (Table 2.1). The absolute difference between rainfall at the low and high elevation sites was consistently between 4 and 9 mm, so the percent difference was smaller for larger events. Rainfall at GC and SG were very similar for all events, suggesting that rainfall was homogeneous for a given elevation. The mean elevation of the watershed is 174 m, with ~58% of the watershed area above the elevation of the HM gage and ~42% below (Figure 2.1). The HM gage is also near the centroid of the watershed, so we use it as representative of mean rainfall over the watershed.

The maximum 15-minute, 1-hour and 6-hour intensities were calculated for each event. The maximum intensity durations were based on the time of concentration (t_c) of the watershed, which was calculated using the Kirpich equation (after Dunne and Leopold, 1978):

$$t_c = \frac{L^{1.15}}{7700H^{0.38}} \qquad (1)$$

where L is the distance from the outlet to the most distant ridge along the main stream (ft), and H is the difference in elevation between the basin outlet and the most distant ridge (ft). At the outlet of LLCW, just south of the US-Mexico border culvert, L=22,326 ft and H=676 ft, so t_c was 1.09 hr.

Table.2.1. Total storm rainfall (mm) at all gages with data. Gage locations are in Figure 1.1.

	Elev m	Total mm	Date range									
Storm #			1	2	3	4	5	6	7	8	9	10
Year			2014	2015	2015	2015	2016	2016	2016	2017	2017	2017
Rain Gage			2/27-3/1	2/28-3/3	5/14-15	9/15-16	1/4-8	3/5-11	4/8-10	1/17-23	2/17-22	2/26-28
RG.GC	36	349	25	27	20	24	44	28	13	59	39	70
RG.SG	40	-	30	-	-	22	46	-	-	58	34	64
RG.HM	174	411	32	36	24	31	50	34	14	65	42	83
RG.RM	187	-	-	-	-	-	-	-	5	-	-	-
SDBF	144	361	30	38	17	22	52	25	19	58	41	59
LIND	5	386	42	26	47	32	76	18	6	48	30	61
IB3.3	40	332	28	35	7	18	53	22	18	47	43	62
HM-GC[a]	-	38	7	9	4	6	7	5	1	6	3	13
%	-	17	26	35	19	27	15	18	6	10	8	18
HM-SDBF[a]	-	50	2	-2	7	9	-2	9	-5	7	1	24
%		14	8	-5	41	41	-3	35	-28	13	2	40
HM-LIND[a]		25	-10	10	-23	-1	-25	15	8	17	12	22
%		6	-24	38	-49	-3	-33	82	131	35	40	36

*. HM-GC, HM-SDBF, and HM-LIND are the difference between rainfall at RG.HM and RG.GC, RG.SDBF, and RG.LIND respectively

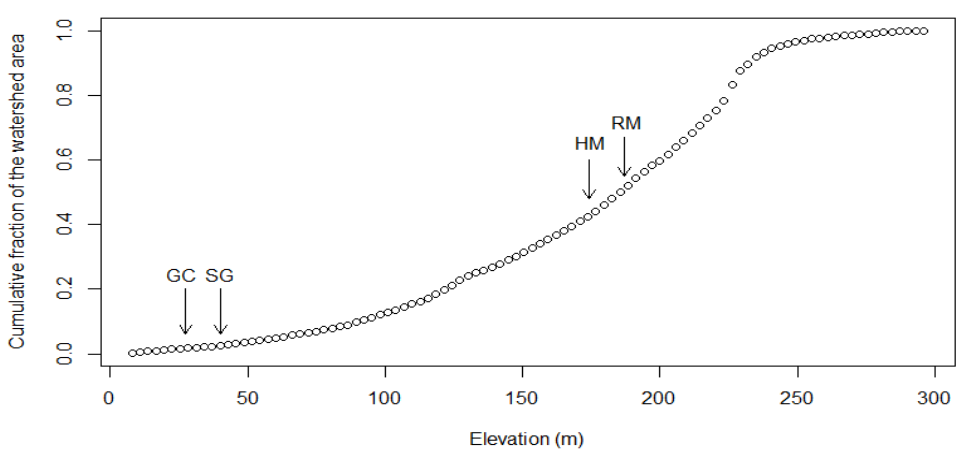

FIGURE 2.1. Hypsometric curve of the LLCW watershed showing the elevation of the rain gages.

2.1.2. Rain gages for sediment traps and modeling

Rainfall data is also required for interpreting the sediment trap data (2005-2014) and for long-term simulation of the runoff and sediment yield of the watershed. The gages for this study only collected data for 2014-2017, and rain gages in Mexico near the LLCW report data only through the 1980s, and so cannot be used for analysis of the sediment trap data.

Several rain gages are maintained in the US by NOAA or the IBWC (Figure 1.1, inset map), though the data availability is variable. Only two stations have 100% data coverage for 2005-2012 (SDBF and Lind) (Figure 2.2), and only one station has 100% coverage for a longer period 1980-2016 (Lind) (Figure 2.3)

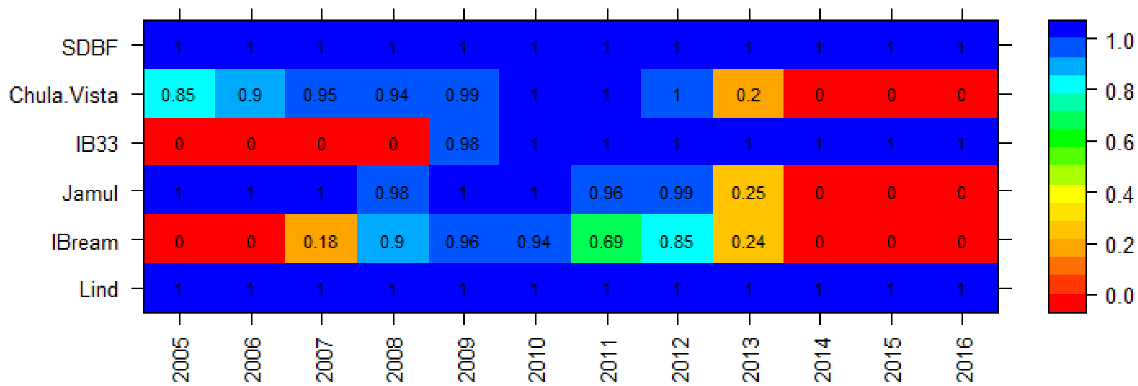

Figure 2.2. Data availability for rain gages near the LLCW over the period when sediment trap data are available (2005-2016). Y-axis is the station, and x-axis is the year. Numbers in the grid indicate the fraction of days with data, out of 365.

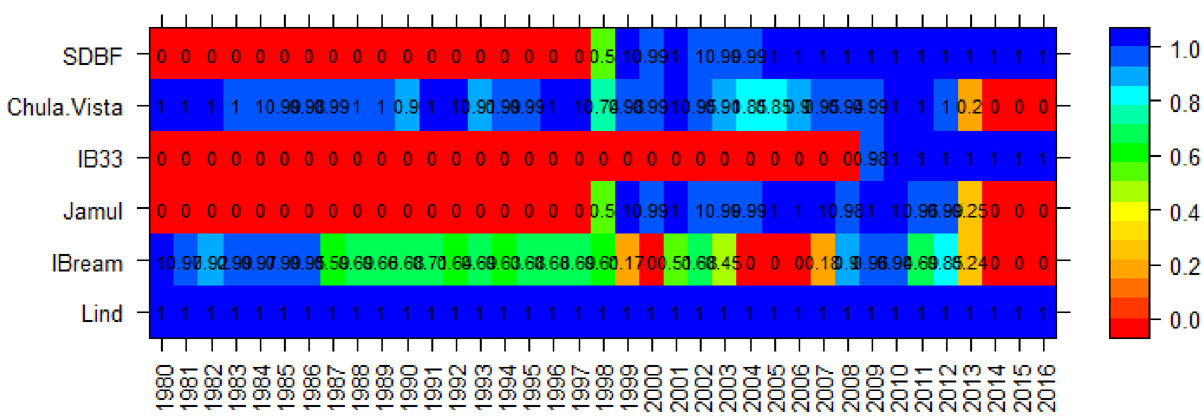

Figure 2.3. Data availability for rain gages near the LLCW over 1980-2016. Y-axis is the station name, and x-axis is the year. Numbers in the grid indicate the fraction of days with data, out of 365.

For the events that have rainfall data in the LLCW watershed at Hormiguitas (RG.HM) (Table 2.1), the gage at San Diego Brownfields (SDBF) has the highest correlation coefficient and smallest

RMSE of the stations with good availability (Figure 2.4). Rainfall at RG.HM was higher than that at all other stations for larger events (>60mm), but matched the SDBF data well for rainfall 10-50 mm (Figure 2.4). The SDBF and HM gages have a higher correlation coefficient and lower error compared with stations closer to the LLCW in the Tijuana Estuary (IB3.3), so SDBF can be considered to be the best available option for estimating rainfall in the LLCW for 2005-2016. Selection of the time series for 1980-2016 for modeling will need to consider the probability distribution of rainfall, which will be analyzed in a future report.

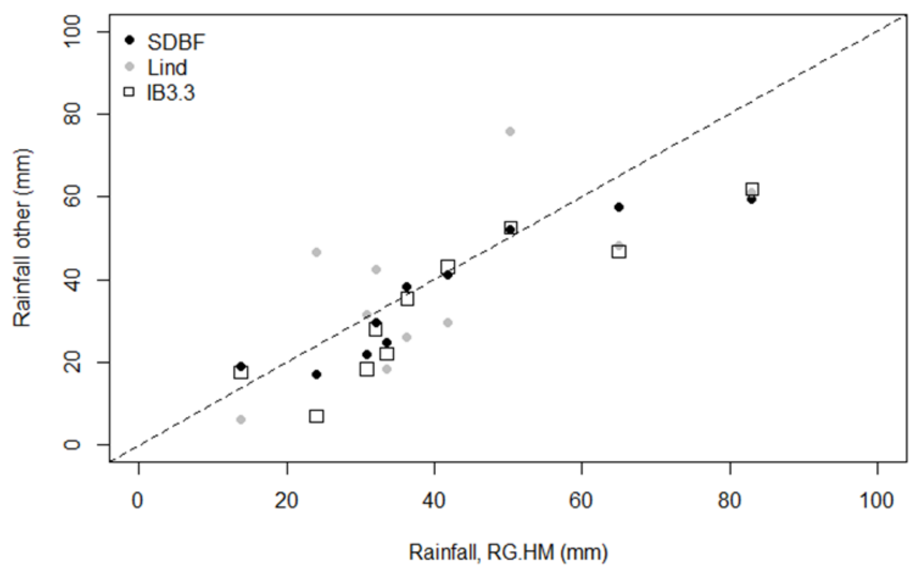

Figure 2.4. Event-total precipitation for the 10 events in Table 2.1 for the RG.HM rain gage versus rainfall for three other nearby stations (SDBF, Lind, IB3.3 in Figure 1.1 inset). The dashed line is the 1:1 line.

2.1.3. Recurrence intervals for measured storms

The recurrence intervals of the rainfall observed at HM were determined by comparing with rainfall depths at 1-10 year return intervals reported in the NOAA Atlas 14 Point precipitation frequency estimates at the Tijuana Estuary (Imperial Beach station) (NOAA, 2017). The recurrence intervals of the largest measured storms at the LLCW ranged from 2-5 years (15-minute, 1 hr) and 5-10 (6 hr) (Table 2.2). Total rainfall at the RG.HM station was 6-32% higher than at the outlet of the LLCW (Table 2.1), so the recurrence intervals may be lower than estimated from the rain gage in the Tijuana estuary

Table 2.2. Rainfall depth (mm) at different recurrence intervals based on NOAA Atlas 14, Imperial Beach station, and the observed 15-minute maximum and median rainfall recorded at the mouth of the LLCW and at the RG.HM station for the 10 monitored storms in Table 2.1.			
	Duration		
NOAA Atlas 14	15 minute	1 hr	6 hr
Recurrence interval (years)			
1	4.5	8.7	19.2
2	5.6	10.9	24.1
5	7.1	13.9	30.5
10	8.4	16.3	35.6
RG.HM max	6.0 (2014-03-01)	11.3 (2015-09-15)	33.3 (2017-02-27)
RG. HM median	3.4	6.3	15.1

2.2. RUNOFF

Water depth was measured at two locations in the main channel near the outlet, upstream of the sediment traps: 1) on the Mexico side of the border, a pressure transducer (PT) was deployed in the main concrete channel (Figure 1.1) before each of the 10 rain events in Table 2.1. The PT was housed in a 4" diameter PVC pipe that extended to the channel bed. In February 2017, a field camera was also deployed at the site to record water depth every 15 minutes during events, in part due to problems with the stability of the PT readings observed during large events. The drainage area at the PT is 10.23 km^2. 2) On the U.S. side of the border, the International Boundary Water Commission (IBWC) maintains a bubbler (Waterlog H350XL pressure sensor and H3551 gas purge system) that records water depth every 15 minutes and transmits data to San Diego County ALERT system (https://sandiego.onerain.com/). The IBWC bubbler is not in an ideal location for discharge measurement, since it is located in a concrete reservoir to the side of the main channel that is separated from the main flow by a set of poles that intercept debris (Figure 2.5), creating possible hysteresis in the stage-discharge relationship. Here, we developed a rating curve for the IBWC gage for a large storm event in February 2017 that had data from the field camera installed in Mexico (Section 2.2.2.2). We then used that rating curve to estimate discharge at the IBWC gage for all events, and compared the IBWC discharge with the discharge recorded by the PT. After events were defined, the rainfall for each event was compared with the Storm Types defined by the Soil Conservation Service (SCS) Technical Report 55 (SCS, 1986). Types I and IA are common in Pacific Maritime climates including California, Type III are typical of tropical storms in Atlantic coastal areas and Gulf of Mexico, and Type II is most common in the rest of the continental United States, and has the highest short-duration (1-6 hr) rainfall intensities.

Figure 2.5. IBWC bubbler located on the side reservoir of the Main channel. Flow from the Main channel passes through the US-Mexico border culverts (A) into the Tijuana Estuary. Photo credit: K. Taniguchi, February 2017.

2.2.1. Pressure transducer and stage correction

2.2.1.1 Atmospheric pressure correction

The PT at the outlet in Mexico measured total pressure (water + atmosphere). In order to calculate water depth, atmospheric pressure from a nearby weather station is subtracted from observed pressure at the PT. For the sampled events, atmospheric pressure data were taken from a nearby barometer, Tijuana Estuary Naval Auxiliary landing field (TJE NAVAL), station USAF 722909, NCDC 93115 in Imperial Beach, CA (https://gis.ncdc.noaa.gov/maps/ncei/cdo/hourly). The station is ~4 km from the outlet of LLCW, but is at the same elevation. Atmospheric pressure at TJE NAVAL and two other nearby barometric stations was higher than total pressure observed by the PTs, though the offset was constant over short (hourly) time intervals (Figure 2.6). For each storm, several offsets were calculated by assuming that water depth was zero after extended periods (~4 to 6 hr) of no rainfall, and the offset was subtracted from the atmospheric pressure time series (Figure 2.6B). The final water level was calculated as the difference between PT total pressure and the adjusted atmospheric pressure at the TJE Naval Base (Figure 2.6). Any negative stage values were replaced with zero.

2.2.1.2 Observed Stage

A staff gage was painted on the side of the channel in January 2016 for comparison with stage calculated from the PTs and atmospheric pressure. Only a few observations were available in 2016 and 2017. On 2016-01-06, video of channel flow was taken at 11:00 am by residents living at the gage location. Based on markings on the channel side, the stage at this point in the January 6, 2016 event was 60 cm, which compares well with the peak stage reported by the pressure transducer (57 cm). See link below for video: https://www.youtube.com/watch?v=lRABWKisSDE&feature=youtu.be

On 2016-03-06 at 9:40 am, the maximum stage verbally reported by residents was 25 cm, compared with a maximum stage recorded by the PT of 6 cm. Stage was also measured with a camera and visually in January and February 2017, but the PT failed so no comparison was possible. Photographs of the channel were taken during water sampling activities on 2014-12-03, 2014-12-12, 2014-12-13, 2014-12-13, 2014-12-17, 2015-03-01, 2015-05-14, and 2017-01-21. The photo taken on 2015-05-14 shows flow in the channel when the PT recorded zero stage, due to a slightly uneven concrete channel bottom that focused flow in part of the channel not in contact with the PT.

More data is needed to validate the stage recorded by the PT. The limited visual stage observations suggested that the PT underestimated water depth by several cm, but insufficient data were available to develop a single correction factor. The proportional error should be smaller for peak discharge assuming that the underestimation is a constant offset of a few cm.

See Appendix A for a complete description of all observed storm events.

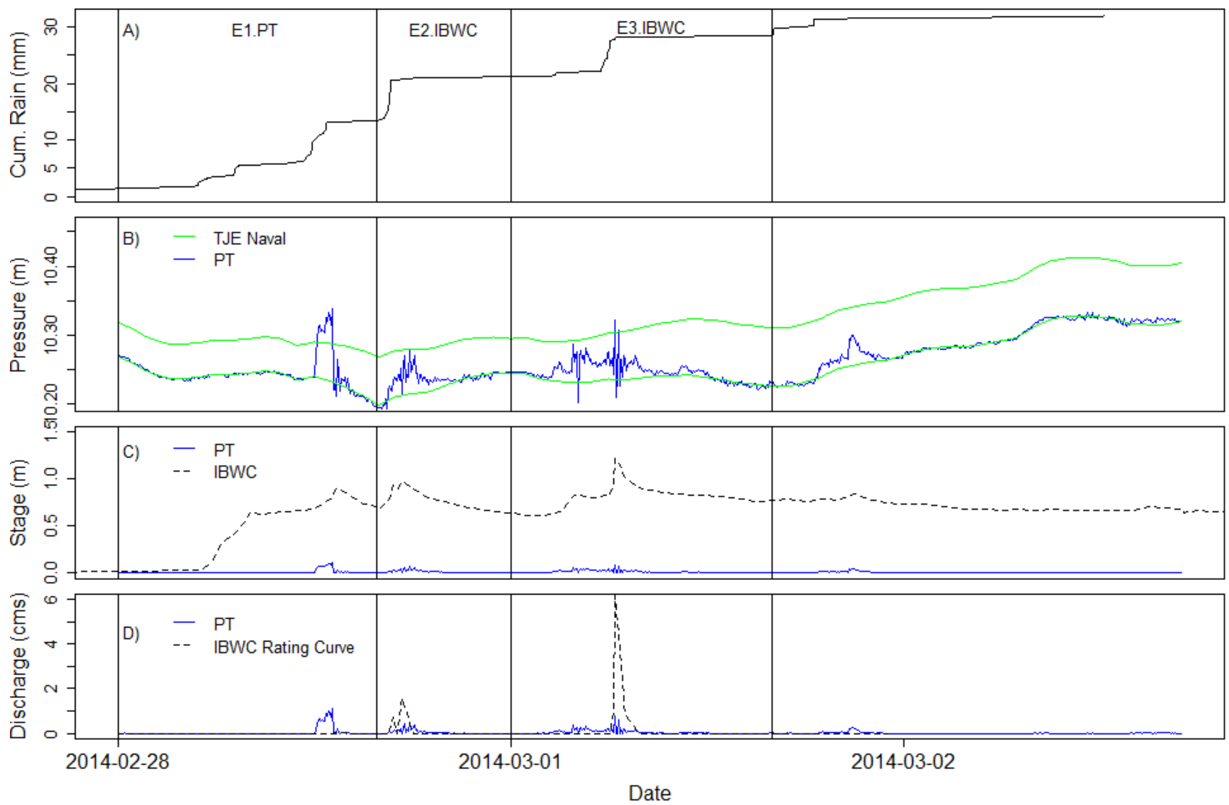

Figure 2.6. Storm 1, 2014-02-28 to 2014-03-02, with A) cumulative rainfall, B) pressure, including atmospheric pressure from the weather station (upper green line), adjusted atmospheric pressure (lower green line), and pressure at the PT (blue), C) water stage, and D) discharge. The vertical lines indicate where events were defined (Table 2.3). E1, E2, and E3 indicate the three events that were retained for the model and validation. In Panel A, ".PT" and ".IBCW" indicate that the PT or the IBWC discharge estimate was selected as the most reliable for that event.

2.2.2. Discharge calculation

2.2.2.1 Discharge from the PT stage

Discharge at the PT was calculated using Manning's equation (Dunne and Leopold, 1978, p. 592), with Manning's roughness coefficient based on field measurements in 2016 and 2017. Velocity was estimated for one discharge event on January 5, 2016 with video and floating debris in the channel: https://www.youtube.com/watch?v=lRABWKisSDE&feature=youtu.be. For that event, Manning's n back-calculated from the observed velocity was 0.013. Velocity was also measured on 2017-02-27 at 7 different times from floating debris, which was used to back-calculate a Manning's n ranging from 0.008 to 0.012. Based on these field observations and the Manning's n for "ordinary concrete lining" (0.013, Dunne and Leopold, 1978), the Manning's n used in all calculations of discharge was 0.013. Sediment accumulated in the reach with the PT after some events, which would increase the Manning's n, thereby decreasing the estimate of discharge. Increasing Manning's n from 0.013 to 0.017 ("concrete and earth channels in best condition") would decrease the calculated discharge by 24%.

2.2.2.2 Discharge from IBWC bubbler updated rating curve

The IBWC developed a stage-discharge rating curve for the IBWC bubbler using HEC-RAS (S. Smullen, unpublished data). An updated rating curve was developed for the IBWC bubbler using discharge calculated from the field camera, using Manning's equation and roughness of 0.013, and field measurements of flow velocity for a large storm event in February 2017. Separate rating curves were developed for the rising and falling limbs of the hydrograph, due to potential hysteresis caused by the side reservoir where the bubbler is located (Figure 2.7). The following rating curve equations were developed for the rising and falling limbs:

$$Q_{rising} = \begin{matrix} 0 & s < 0.91\,m \\ 19.6s - 17.76 & s > 0.91\,m \end{matrix} \tag{2}$$

$$Q_{falling} = \begin{matrix} 0 & s < 0.98\,m \\ 21.2s - 20.77 & s > 0.98\,m \end{matrix} \tag{3}$$

where *s* is the stage at the IBWC BBLR (Figure 1.1). The IBWC BBLR provided reliable estimates of discharge only for the largest events, or for smaller events that were preceded by another event that filled the small reservoir that houses the IBWC bubbler. For example, see Figure A9, Storm #6, when the first event (6.5 mm) produced runoff at the PT but an insufficient increase in water level at the IBCW bubbler to result in a non-zero estimate of discharge, while the subsequent event (23 mm rainfall) produced a rise in water level sufficient to result in an estimation of discharge from the PT-IBWC rating curve (Eq 2 and 3). The PT appeared to record reliable stages during small events, but fluctuated erratically for larger events, so for larger events, the IBWC gage and PT-IBWC rating curve were used. See Table 2.3 for which stage reading was used to calculate discharge for each event, and Appendix A for detailed comparison of the PT and IBWC data.

Table 2.3 Summary of storm events defined in Table A1, final observed data (obs) used for calibration/validation. TCM = thousand cubic meters.

Event Date*	Rainfall (mm)	Peak Discharge (cms)	Total Runoff		Runoff Ratio (Q/P)	Event	Source
		Obs	Obs (mm)	Obs (TCM)	Obs		
Storm 1							
2014-02-28	12.25	1.13	0.27	2.80	0.02	E1	PT
2014-03-01	7.50	1.54	0.33	3.36	0.04	E2	IBWC
2014-03-02	7.50	6.14	1.08	11.04	0.14	E3	IBWC
Storm 2							
2015-03-01	23.25	3.36	1.36	13.88	0.06	E1	PT
2015-03-02	9.25	1.43	0.48	4.86	0.05	E2	PT
Storm 3							
2015-05-15	22.50	19.46	5.93	60.63	0.26	E1	PT
Storm 4							
2015-09-15	30.75	5.27	6.40	65.50	0.21	E1	PT
Storm 5							
2016-01-05	22.25	17.72	3.76	38.42	0.17	E1	PT
Storm 6							
2016-03-06	6.50	1.03	0.93	9.47	0.14	E1	PT
2016-03-07	23.00	5.07	4.23	43.32	0.18	E2	IBWC
Storm 8							
2017-01-19	13.00	5.37	2.57	26.27	0.20	E1	IBWC
2017-01-20	28.00	6.86	18.66	190.95	0.67	E2	IBWC
Storm 9							
2017-02-17	33.25	11.16	7.03	71.89	0.21	E1	IBWC
Storm 10							
2017-02-27	83.00	16.69	42.07	430.50	0.51	E1	CAMERA

*For storm 7, no PT data were available and IBWC rating curve discharge was zero.

Future work could attempt to extend the PT-IBWC rating curve for lower discharges, though the rating curve for low discharges will be complicated by hysteresis as the reservoir containing the IBWC bubbler fills during and empties after events. An alternative would be to install a bubbler closer to the outlet of the channel, on the channel side of the debris barriers (to the right of the yellow debris catch poles in Figure 2.5).

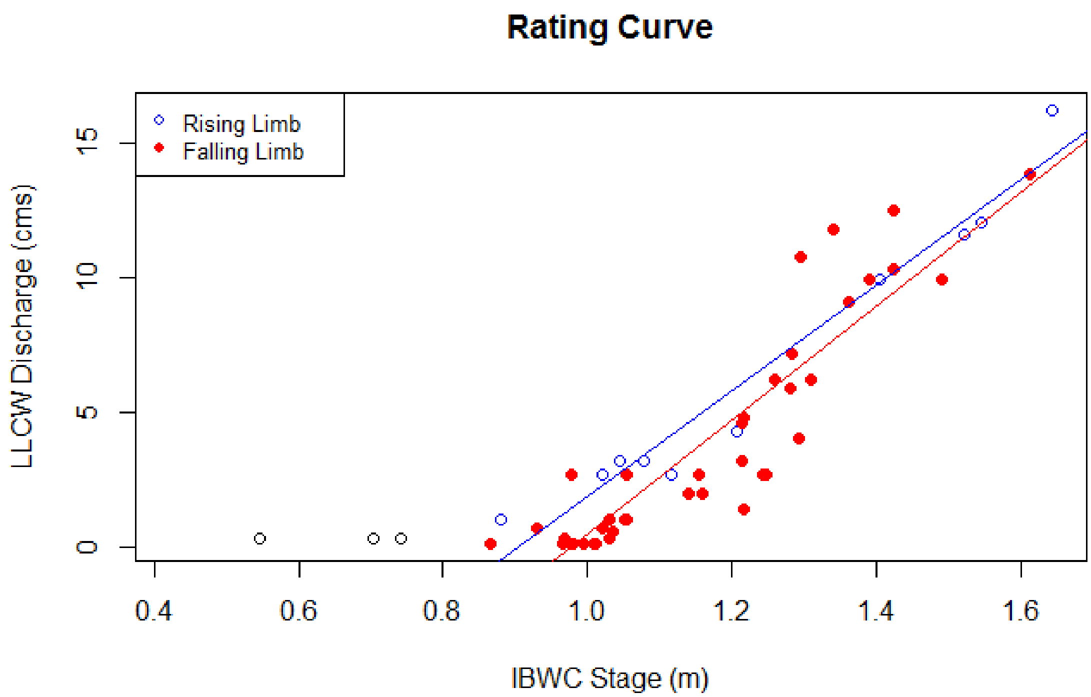

Figure 2.7. Rating curves developed for the rising (blue) and falling (red) limbs of the hydrograph based on the relationship between IBWC bubbler stage and LLCW camera discharge for Storm 10 (2017-02-27). The text refers to this relationship as the PT-IBWC rating curve.

2.2.3. Event determination

During each storm, multiple rainfall and runoff events occurred over several days (e.g. Figure 2.6). Future work will use the AnnAGNPS model, which assumes only one single rainfall/runoff event occurs per day. Data on rainfall and runoff on days with multiple rainfall and runoff events were split and re-assigned to subsequent days so that a single event occurs on each day, which facilitates comparison of modelled and observed event discharge.

Events can be defined by the number of hours between rainfall events, by the discharge time series. Since the AnnAGNPS model requires that there be only one single rainfall event a day, we divided the hydrograph into separate events, and assigned a single event to each day. In some cases, that resulted in removal of an event from the time series (e.g. the small event following E3.IBWC on 2014-03-01 in Figure 2.6). After reallocating rainfall to have only one event on the day that rainfall occurs, any remaining rainfall was allocated to the following day but was not used in the analysis of rainfall-runoff relationships (e.g., see adjusted rainfall for 2014-03-03 in Table A1).

This event identification strategy resulted in 14 events during the 10 storms over the study period (Table 2.3). Reallocation of rainfall and runoff data for all storms is described in Appendix A (Table A1). Table A2 presents runoff for both PT and IBWC gages.

Example of Event Determination: Storm 1, 2014-02-28 to 2014-03-02

There were four distinct runoff events over this storm period (Figure 2.6). The two events on 2014-02-28 were divided into two separate events, the first on 2014-02-28 and the second 2014-03-01, and the third event was set to 2014-03-02 (Table 2.3). The fourth event was small and excluded from the model calibration and validation. Event 1 did not fit any storm type as defined by the Technical Release 55 (TR-55: Soil Conservation Service, 1986), but was adequately modeled by storm Type 2, 12 hour (Figure 2.8).

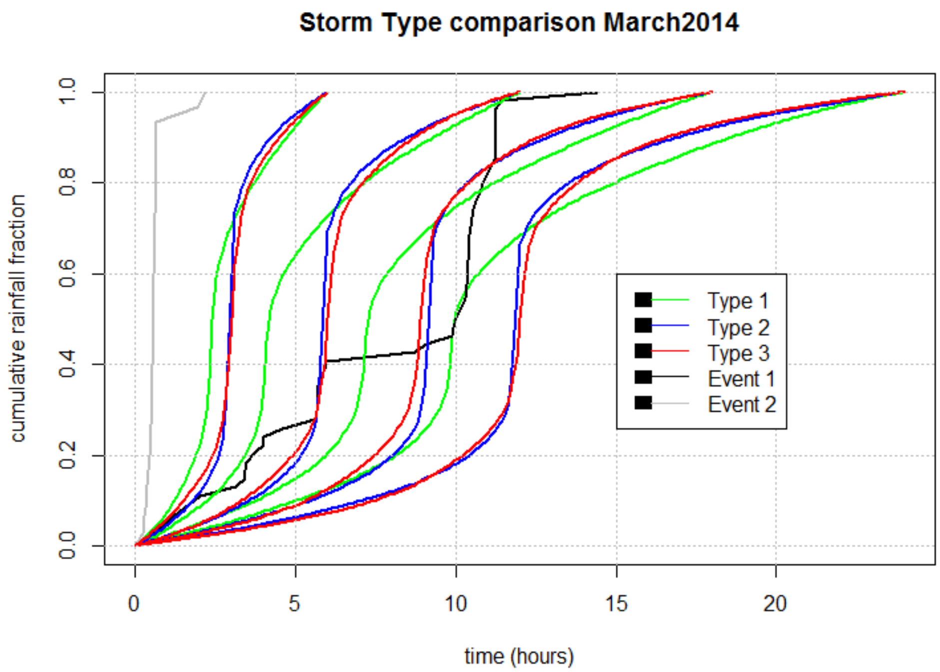

Figure 2.8. Cumulative rainfall fraction, normalized to storm total rainfall, for the two events in March 2014. The four groups of three lines correspond to the 6-hour (left-most group), 12-hour, 18-hour, and 24-hour design events from TR-55 (Soil Conservation Service, 1986).

2.2.4. Rainfall-runoff relationships

Event rainfall for the 14 events ranged from 7 to 83 mm. The 6-hour rainfall intensity ranged from 1.5 to 33.3 mm. The 1-hour intensity ranged from 0.5 to 11.3 mm, and the 15-minute intensity ranged from 0.25 to 6.0 mm.

Event total runoff increased with event-total rainfall (Figure 2.9). The runoff coefficients (Q:P) ranged from 0.02 to 0.67 (Table 2.3). The largest event (rainfall 83 mm) had a runoff coefficient of 0.51. Most events fell between SCS Curve Numbers (CN) 80 and 90 (Figure 2.9), which is consistent with the urban land cover in the watershed. The CN was highest for the smallest events and generally decreased with event size. This is consistent with runoff production from surfaces with low infiltration capacity during small events, and from all surfaces, including those with high infiltration capacities, during large events.

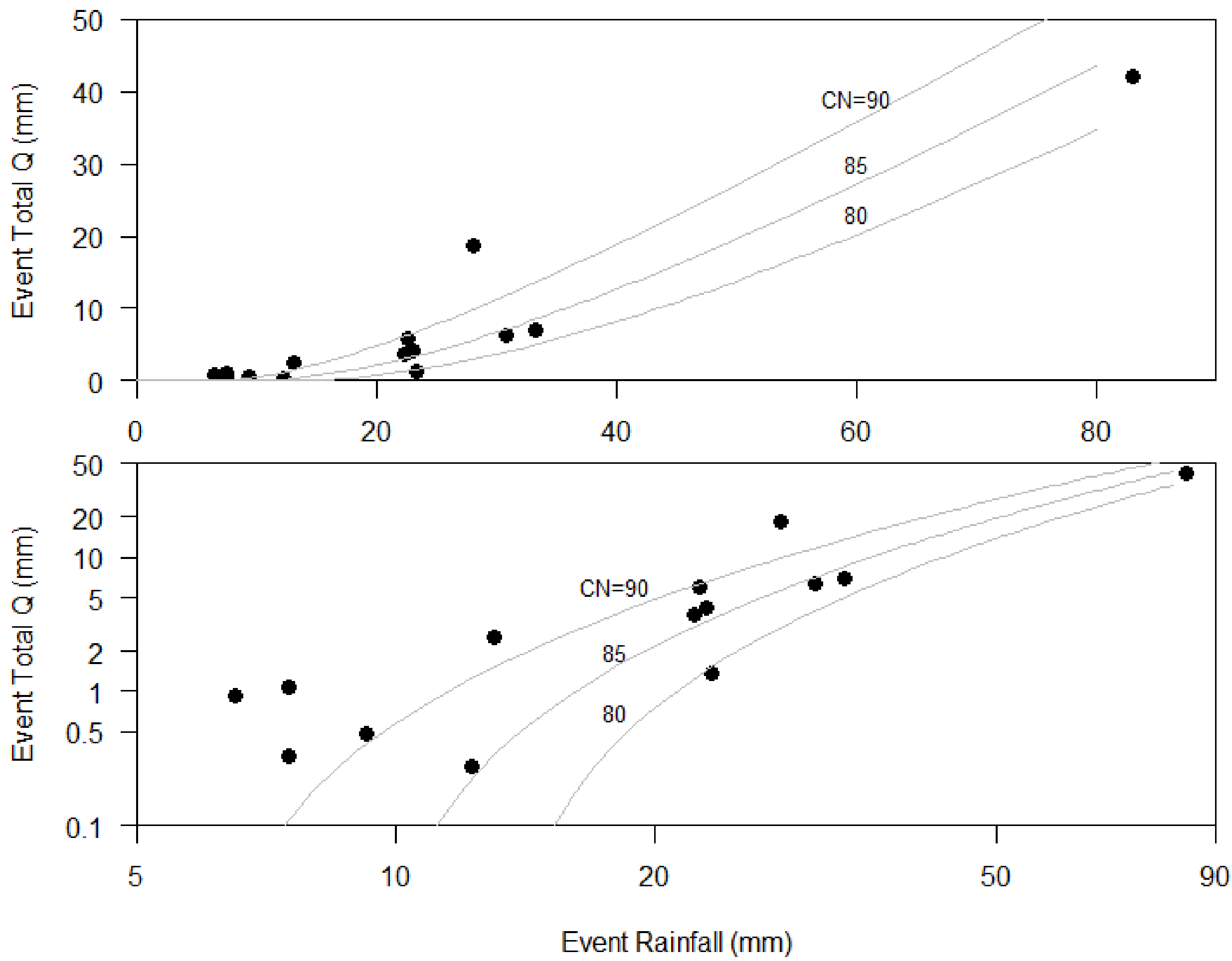

Figure 2.9. Rainfall-runoff relationship for all observed storm events summarized in Table 2.3, with several SCS CN rainfall-runoff relationships, in non-log (top) and log-log (bottom).

Peak event discharge (Qpk) was predicted better by the event-maximum 6-hour rainfall intensity (Pearson r 0.71, $p<0.01$) than by the total event rainfall (Pearson r 0.58, $p<0.05$) (Figure 2.10), mostly due to two high-Qpk outliers. Qpk was not predicted well by the 15 minute ($p>0.1$) or 1 hour ($p>0.05$) maximum intensity rainfall.

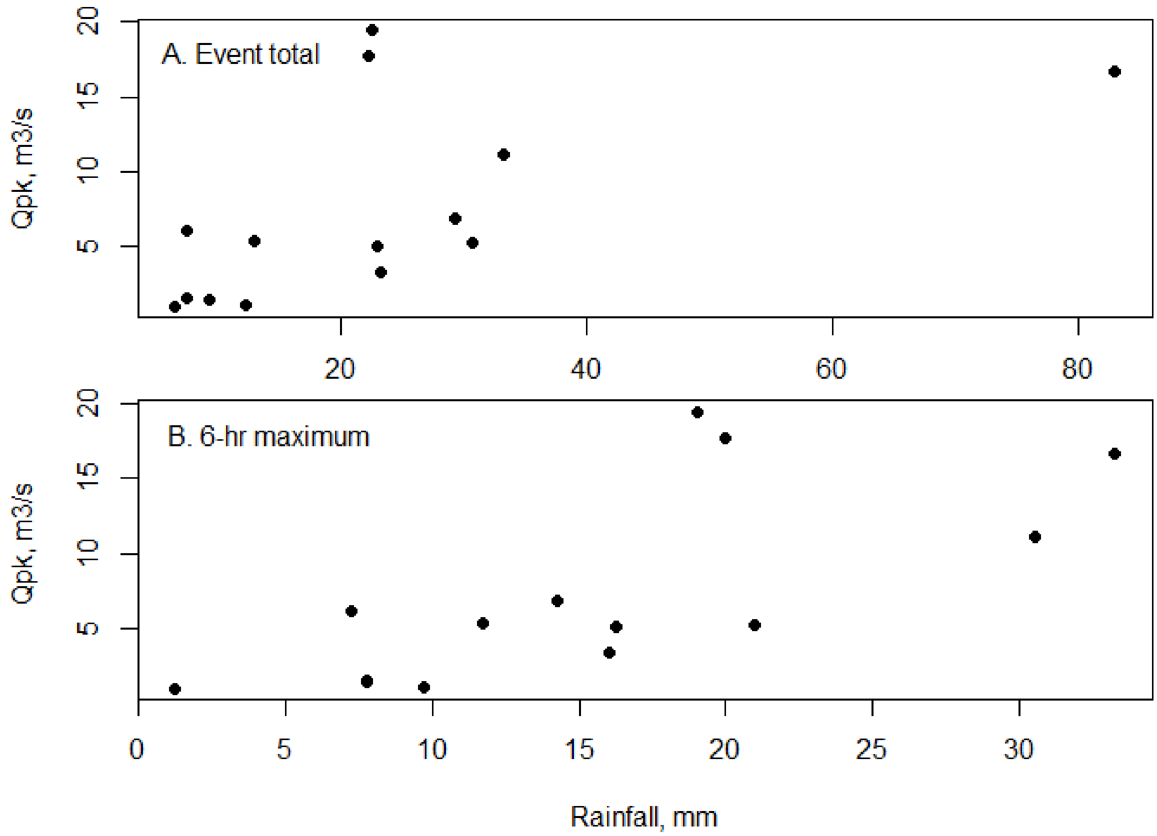

Figure 2.10. Peak event discharge (Qpk) versus: A. event total precipitation and B. 6 hour maximum precipitation for the events in Table 2.3.

2.3. Suspended sediment concentrations and event-wise loads

2.3.1 SSC measurements and SSC-Q relationships

Water samples were collected using grab sampling during storm events at the outlet of the watershed. Due to the high flow velocities and/or small water depths at the time of sampling (often < 30 cm), it was not possible to use a depth-integrated sampler, so a surface grab sample was taken. The water samples were filtered using pre-weighed filters with nominal pore size of 0.45 µm that were then dried and reweighed to calculate the suspended sediment concentration (g L^{-1}). Discharge estimated at the PT was zero for some SSC sampling times due to the position of the PT on the side of the channel. Based on photographs taken during the SSC samples, an estimated minimum discharge (Qmin) at the time of SSC sample collection was 0.07 m^3/s, which corresponds to 2 cm of flow depth. All discharge values less than 0.07 m^3/s at the time of SSC sampling were assumed to be equal to Qmin.

The relationship between SSC and Q was highly variable at low discharges (<0.1 m^3 s^{-1}) (Table 2.4, Figure 2.11). SSC during relatively low discharges was high (> 18 g L^{-1}) and was only slightly lower than the maximum observed SSC (27 g L^{-1}). The variation in the SSC-Q relationship could not be ascribed to hysteresis in the SSC-Q relationship because no event included samples on both the rising and falling limbs of the hydrograph, and because low concentrations were observed both before and after the peak (Appendix B).

Table 2.4. Suspended sediment concentration (SSC) for all collected samples.

Storm	Date	SSC (g L^{-1})	Q (m^3 s^{-1})
Storm 1	2014-02-28 17:20:00	3.23	1.54
	2014-03-01 07:40:00	0.35	0.07*
Storm 2	2015-03-01 07:20:00	15.20	0.33
	2015-03-01 12:40:00	19.40	0.07*
	2015-03-01 17:45:00	13.70	0.07*
	2015-03-02 08:40:00	3.20	0.07*
Storm 3	2015-05-15 08:30:00	15.85	0.14
Storm 6	2016-03-06 09:40:00	16.34	0.42
	2016-03-06 12:00:00	14.58	0.39
	2016-03-06 15:45:00	18.53	0.11
	2016-03-07 06:00:00	15.21	0.07*
	2016-03-07 07:00:00	16.37	0.07*
	2016-03-07 12:00:00	11.70	0.07*
Storm 9	2017-02-17 16:00:00	0.22	0.07*
	2017-02-17 17:00:00	0.23	0.07*
	2017-02-17 20:30:00	20.01	4.11
Storm 10	2017-02-27 12:37:00	15.56	9.91
	2017-02-27 13:13:00	21.93	5.52
	2017-02-27 13:34:00	27.02	6.18
	2017-02-27 14:00:00	24.13	4.00
	2017-02-27 14:05:00	10.98	4.00
	2017-02-27 14:30:00	20.83	7.97
	2017-02-27 15:00:00	14.44	6.18
	2017-02-27 15:35:00	24.81	2.67
	2017-02-27 16:02:00	11.51	2.67

* Recorded Q was <0.07 m^3 s^{-1} (stage of <0.02 m); assumed minimum water depth of 0.02 m and Q of 0.07 m^3 s^{-1}.

The exponent on the relationship between Q and SSC (0.32) was lower than observed in most other watersheds in the literature, where b ranges from 0.38 to 2.0 (Syvitski et al, 2000). Relatively flat rating curves as observed in the LLCW are indicative of highly erodible material that can be transported for a wide range of flows (Asselman, 2000).

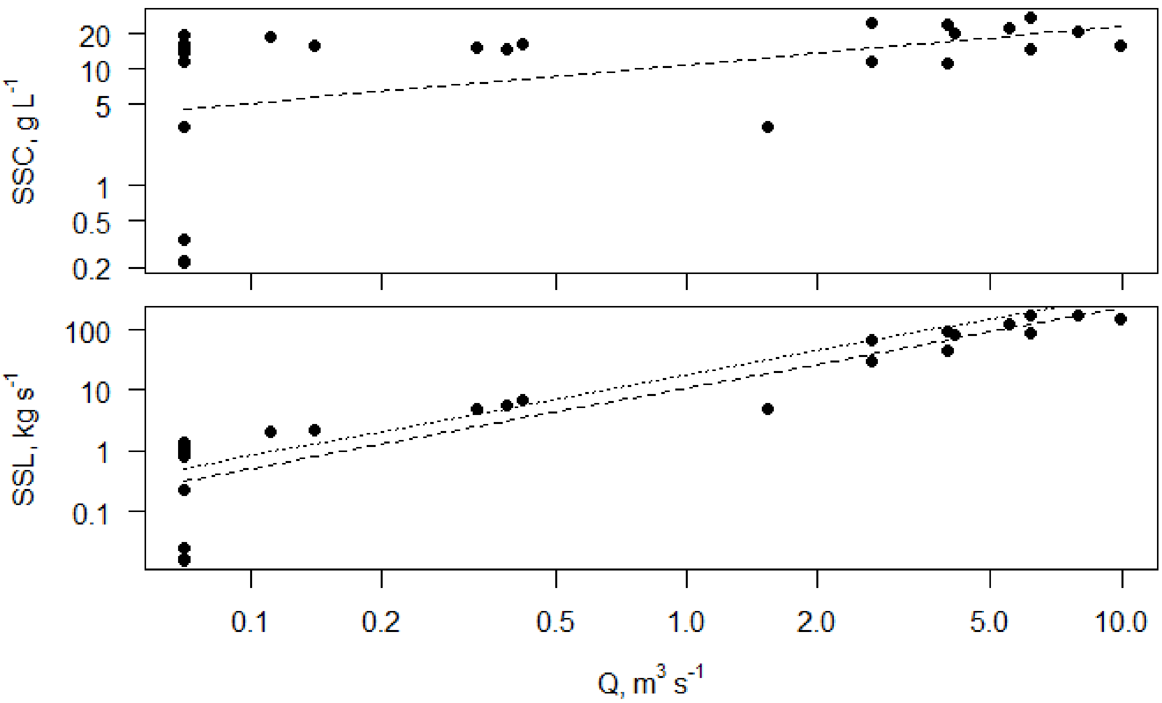

Figure 2.11. Relationship between discharge (Q) and suspended sediment concentration (SSC) and suspended sediment load for the samples collected in the LLCW. The dashed line is the linear regression fit without bias correction, and the dotted line in the Q-SSL plot is with bias correction.

2.3.2. Event-wise suspended sediment loads (SSL)

The suspended sediment load (SSL) was calculated for each event with SSC data using four methods: 1) as the product of the event total discharge and the volume-weighted-mean (VWM) of SSC of the individual grab samples for that storm, 2) as the product of the event total discharge by the VWM SSC for all samples from all storms, 3) using the Q-SSL rating curve (Figure 2.11) to estimate SSL for each 15-minute discharge value during the storm, and 4) using the same rating curve approach as in 3), but with the bias correction factor (bcf) as described by Crawford (1991), which is based on the suggestion of Duan (1983). The bcf corrects for the underestimation of SSC the results from the use of ordinary-least squares on log-transformed data.

The SSL varied over two orders of magnitude for the observed storms (Table 2.5). SLL varies by a factor of ~2 depending on the method used to calculate it, with a factor of 5.6 difference for one storm on 2014-02-28.

Table 2.5. Total event suspended sediment concentration (SSC) and load (SSL) at the PT location for the events with SSC data.

Event	N SSC	Total Q		SSC[a]	SSL (tons)			
		Mm	TCM	g L^{-1}	Event VWM[b]	All VWM[c]	Rating, no bcf[d]	Rating, bcf[e]
2014-02-28 E2	1	0.3	3.4	3.2	11	62	35	56
2015-03-01 E1	3	1.3	13.8	15.2	209	255	151	246
2015-05-15 E1	1	5.9	60.5	15.8	958	1118	1408	2289
2016-03-06 E1	3	0.9	9.1	15.9	144	168	78	126
2017-02-17 E1	3	7.0	71.9	20.0	1438	1329	1356	2204
2017-02-27 E1	9	42.1	430.6	19.0	8199	7961	8657	14073

[a] Volume-weighted mean suspended sediment concentration.

[b] = Q x VWM (volume weighted mean SSC concentration) for samples collected during the event.

[c] = Q x VWM (volume weighted mean SSC concentration) for all samples, all events.

[d] Calculated from the Q-SSL rating curve, with no bias correction factor.

[e] Calculated from the Q-SSL rating curve, with bias correction factor.

2.3.3. Particle size distribution of SSC samples

The particle size of three SSC samples from April 2016 were analyzed on a laser particle size analyzer. The time was not recorded for these samples by the in-field volunteer collectors, so their relationship to the hydrograph is unknown. They have a large silt percentage (70-80%, Table 2.6). The particle size from this and other events will be compared to the texture of soil in the watershed in future reports.

Table 2.6. Particle size of SSC samples collected in April 2016. Time and discharge for the collection is unknown.

Type	Diameter (µm)	Sample 1 (%)	Sample 2 (%)	Sample 3 (%)
Medium sand	250-500	0	0	0.2
Fine sand	125-250	2.6	0.8	4
Very fine sand	63-125	10.5	5.5	10.7
Silt	4-63	73.5	79.4	75.7
Clay	<4	13.4	14.3	9.4
Median (µm)		10.5	5.5	9.4

2.4. SEDIMENT LOAD IN TRAPS AT THE OUTLET

The two sediment traps in the United States (Figure 1.1) were completed in late 2004. Data on sediment removed from the traps were available from the Tijuana River National Estuarine Research Reserve (TRNERR). Both upper and lower traps were cleaned out in spring and fall 2005, winter 2006, and each fall from 2007-2012. Starting in 2013, the lower trap was not excavated due to low rainfall

(Table 2.7). Topographic surveys were conducted in Fall 2011 (both upper and lower traps) and Fall 2015 (upper trap only).

Table 2.7. Time series of sediment removed from LLCW (Goat Canyon) traps. Data from Chris Peregrin and Cara Stafford at TRNERR. Mass is calculated using bulk density of 1.67 tons m^{-3}. TL=based on truck loads, CE=complete excavation. UP=upper basin only excavated. PE=partial excavation, NE =no excavation either basin.

Removal date	Volume removed (yd^{-3})	Mass removed (tons)		Trap efficiency	Notes
		Uncorrected	Corrected		
2005-03	55,000	-	-		TL, CE
2005-10	35,000	-	-		TL, CE
2006-12	25,000	31920	34642	0.92	TL, CE
2007-10 or -11	25,000	31920	33079	0.96	TL, CE
2008-09	40,000	51072	64580	0.79	TL, CE
2009-10 or -11	45,400	57967	68949	0.84	TL, CE
2010-09 or -10	55,000	70224	78935	0.89	TL, CE
2011-09	50,733	64776	70965	0.91	URS/NV5 survey, CE
2012-09 or -10	45,000	57456	58513	0.98	TL, CE
2013-09 or -10	14,967	-	-		UP, PE
2014-09 or -10	0	-	-		NE
2015-09 or -10	17,963	-	-		Rick Engineering survey: UP, PE
Mean		52190	58523	0.89	

Trap efficiency and corrected sediment load

The total sediment yield includes sediment retained in the trap and sediment that flowed through the trap and entered the estuary. The trap efficiency, which is the proportion of the total sediment yield that is retained in the sediment basin, was calculated based using Urbonas and Stahre (1993), which is for turbulent and non-ideal conditions:

$$E = 1 - \left[1 + \frac{1}{n}\frac{\omega}{\omega_c}\right]^{-n} \tag{4}$$

where E (range 0 to 1) is the trap efficiency of the sediment in the size class corresponding to particle fall velocity ω; ω_c is the critical velocity of the basin, which is the fall velocity of the smallest particles that are 100% retained; and n is a factor that depends on the hydraulic efficiency of the basin. A range of n values (n = 1 and n = 3) was used in calculating trap efficiency, where n = 1 represents poor settling conditions and n = 3 represents good settling conditions, both for turbulent and non-ideal conditions (Morris and Fan, 1998). Turbulent and non-ideal conditions were used to give a lower-bound estimate of the trap efficiency. Methods for calculating ω and ω_c are in Appendix C.

The trap efficiency varies by particle size, storm event and year. A mass-weighted annual trap efficiency was calculated for each year and particle size as:

$$E_{ann} = (\sum Q_i E_i) / \sum Q_i \qquad (5)$$

where Q_i is the mean daily discharge on day i and E_i is trap efficiency on day *i*. Daily Q was estimated from a coupled AnnAGNPS-CONCEPTS model (in preparation). The resulting E_{ann} by size class allowed for correction of the observed sediment loads to a total sediment load by size class. Corrected load was calculated by using n=3 for E_{ann}, representing good settling conditions. The particle distribution was taken from that observed in the upper sediment trap (AMEC, 2007) (Appendix C). More than half of the sediment in the traps is sand (Table C1), and the median grain size is fine sand. There was no statistical difference in median particle size between the upper and lower basins, so the upper basin was used to calculate the trap efficiency. de Temple et al. (1999) reported somewhat more sand in surface samples of the estuary near the LLCW outlet (Table C1).

The annual trap efficiency varied from 0.79 to 0.98, and was 0.89 for the cumulative mass removed over 2006-2012 (Table 2.7). Details of the trapping efficiency by particle size are in Appendix C (Table C2).

Total sediment accumulation in the traps correlates with precipitation at both Lindbergh Field (Lind) and San Diego Brownfields stations (Figure 2.12). The relationship is linear, which is unexpected given the usually non-linear relationship between rainfall and sediment load (Inman and Jenkins, 1999).

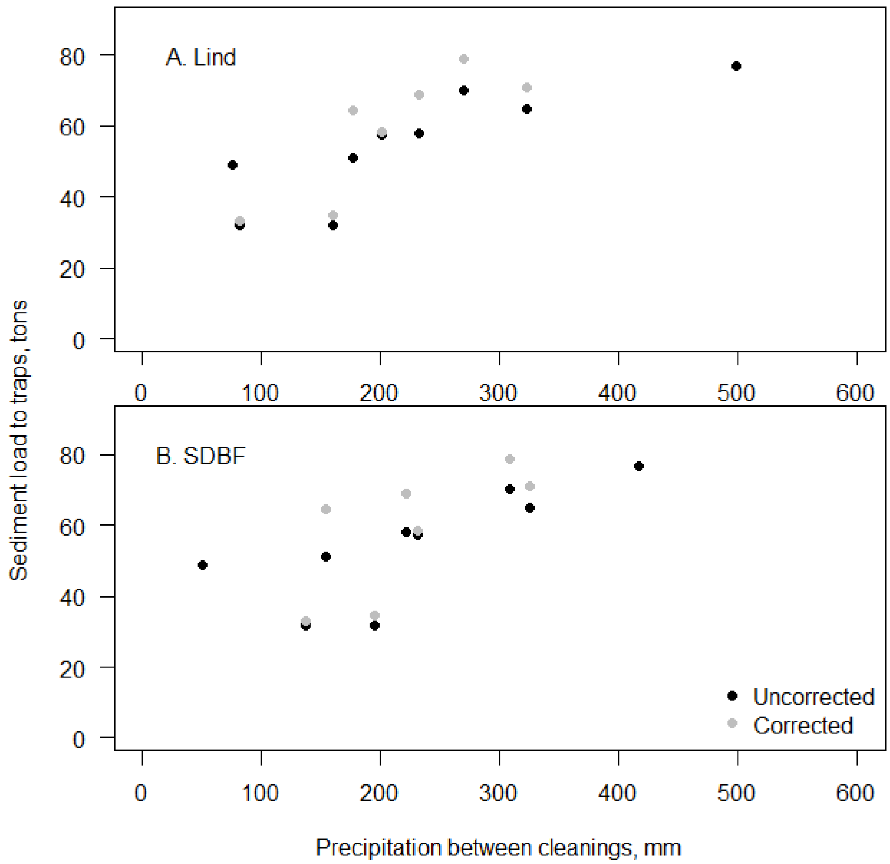

Figure 2.12. Sediment load to the LLCW (Goat Canyon) sediment traps traps versus total precipitation between cleanings, 2005-2012. The uncorrected values (black) are the tons of sediment removed from the trap between cleanings, and the corrected values (grey) are calculated using the retention efficiency for each particle size class (sand, silt, clay). Precipitation is from A. Lindbergh and B. San Diego Brownfields station.

2.5. Sediment accumulation in retention basin in Mexico

A retention basin was installed in the main channel of LLCW during the project period (2012-2014, Figure 2.13) downstream of the confluence of the main and southeast channel, but upstream of the confluence of the main and southwest channel (Figure 1.1). The basin dimensions are approximately 25-33 m wide, 5-6 m deep, and 172 m long. Based on Google Earth imagery, construction began in November 2012 (outlet structure was built), concrete was poured in winter 2013-14, and the project was finalized by July 2014.

Figure 2.13. Soil depth survey in the Mexico sediment basin in LLCW, taken on January 15, 2016. The sedimentation basin was installed in winter 2013-14. Yellow pins indicate locations of depth measurements (Table 2.8) and blue drop symbols indicate the locations of soil sample collection for particle size analysis (Table 2.9).

2.5.1. Sediment survey after storm in January, 2016

Following the storm from January 4-8, 2016 (total rainfall 49.8 mm), sediment accumulated in the new retention basin. A survey of sediment depth was conducted after the storm (Figure 2.13, Table 2.8). Sediment depth was fairly uniform in the basin, ranging from 33-64 cm, with a mean depth of 55 cm. The total sediment accumulation during the event was approximately 3,600 tons. The total sediment yield at the outlet of the watershed at the US-Mexico border estimated from the VWM for all samples as in Section 3.2 is 38.42 thousand m^3 x 18.5 g/L = 711 tons, or just 20% of what was retained in the Mexico trap. This could indicate that either the sediment retained in the trap represented a significant fraction of the total watershed load, or that the load estimated from the VWM is an underestimate. Future sampling and comparison with sediment accumulation in the traps in Mexico and the US will help substantiate the sediment budget and the impact of the Mexico trap.

2.5.2. Particle size distribution in the sediment trap in Mexico

Samples of sediment that accumulated in the retention basin were collected on January 15, 2016 and analyzed for particle size distribution on a laser particle analyzer at UABC, Ensenada. The samples were dominantly very fine to fine sand, with very little clay (Table 2.9, Figures 2.14 and 2.15).

Table 2.8. Sediment depth at the new retention basin on January 15, 2016. IDs correspond with Figure 2.13.	
ID	Sediment depth (cm)
1	33
2	55
3	Cobble
4	63
5	55
6	64
7	62
Mean	55

Table 2.9. Particle size of sediment samples in the sediment trap in Mexico, January 2016. All samples taken from 2-10 cm depth. Samples had no gravel or cobble. Location codes correspond to Figure 2.13.					
Location code	Lab code	Photo Figure	Particle size percentage (%)		
			Sand 0.063-2mm	Silt 4-63 um	Clay <4um
8.1	9	C4	79.2	18	2.8
8.2	10	-	74.2	23	2.8
8.3	11	-	78.2	19	2.8

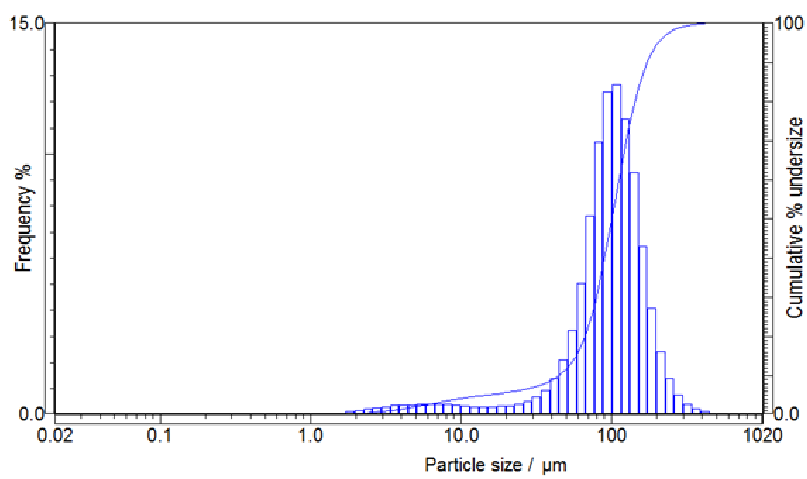

Figure 2.14. Particle size distribution at the sediment basin (location code 8.1)

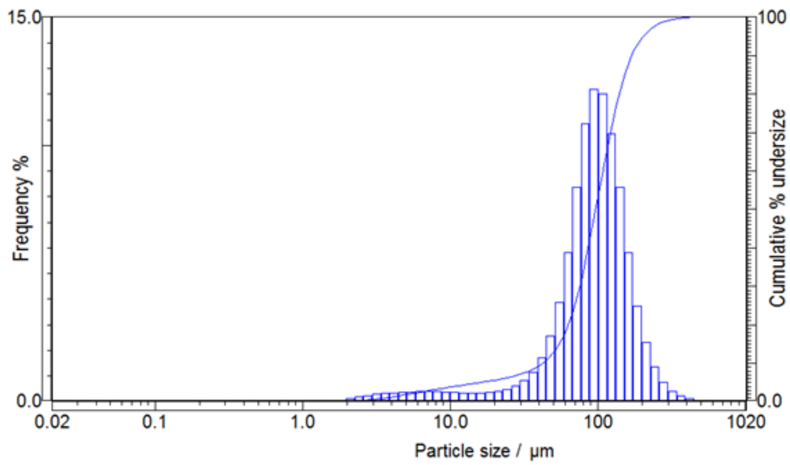

Figure 2.15. Particle size distribution at the sediment basin (location code 8.3). Silt is 3.9-62.5 um on the phi scale. Very fine sand is 62.5-125 and fine sand is 125-250 um.

3. DISCUSSION

3.1. RAINFALL AND RUNOFF

The rainfall events fit a mix of type I (N=6) and type II (N=7) storms (Appendix A), as defined by SCS (1986). Type I storms are typical of Pacific Maritime climates, with lower storm intensities over short durations. Type II events are typical of the rest of the continental United States outside the Gulf Coast, and have the highest short-duration intensities. Our data suggest that both high-intensity type II and low-intensity Type I storms can occur in the study area, with some storms showing short durations and high intensities (e.g. 6T2). The relationship between storm characteristics and key driving mechanisms and moisture sources is not determined here but would be helpful for future research, since storm type can influence key attributes of watershed response, including storm runoff, peak discharge, and sediment generation.

The event-total rainfall and runoff for the observed events are consistent with an SCS CN of between 80 and 90, with decreasing CN for larger events (Table 3.1). The hydrologic soil group of the LLCW is assumed to be type B based on the soil type (cobbly sandy loam and sandy loam), but in places may be a type C that has an impeding layer. The CN range for the observed events in the LLCW is consistent with the CN for urban land use with an impervious cover of between 30 and 65%, compared with impervious cover in the LLCW of ~30%. Soil moisture is critical for runoff production in semi-arid watersheds, so more detailed modeling that accounts for soil moisture impacts on runoff production may explain variation in runoff among events.

Table 3.1. SCS Curve numbers (CN) from the literature (Dunne and Leopold, 1978 Table 10-8) and for the LLCW.		
	Hydrologic Soil Group	
	B Moderate infiltration rate, moderately deep to deep, moderately fine to moderately coarse textures	C Slow infiltration rates when wetted; often have impeding layer, or moderately fine to fine texture
Residential, 65% impervious	85	90
Residential, 38% impervious	75	83
Residential, 30% impervious	72	81
Dirt road	82	87
LLCW, ~30% impervious	~80-90	

3.2. SEDIMENT YIELD AT THE OUTLET

The observed sediment yield in the LLCW (4-5 kt km^{-2} y^{-1}) was higher than almost all measured yields from small watersheds in California (Table 3.2), though the sediment yield from undisturbed chaparral land cover on erodible sedimentary formations in the Western Transverse Range can be as high as 5.3 kt km^{-2} y^{-1} (Warrick and Mertes 2009). An urbanized watershed in southern California (drainage area 288 km^2) with severe channel erosion yielded 0.5 kt km^{-2} y^{-1} (Trimble 1997), which is 10% of the yield from LLCW, though Trimble (1997) did not report gully formation on hillslopes, which was a major process generating sediment in the LLCW.

The high sediment yield from the LLCW was due in part to the high urban cover percentage (86%) that has a high (30-40%) bare soil cover fraction (Biggs et al, 2010), including construction sites and unpaved roads that showed signs of severe erosion, including rills and gullies. A global survey (Russell et al, 2017) shows that construction sites have between 21 and 11,613 times the sediment yield of the undisturbed background, and that urban areas can have 1.7 to 68 times the sediment yield as the background. Unpaved roads also have very high sediment yields, including 125 kt km^{-2} y^{-1} for heavily-used logging roads in the Pacific Northwest (annual rainfall 390 cm) (Reid and Dunne 1984) and 11 kt km^{-2} y^{-1} for recently graded roads in the US Virgin Island (annual rainfall 115 cm). Given that unpaved roads in the LLCW showed signs of severe erosion similar to what was observed on construction sites, the observed range of 4.5-5.0 kt km^{-2} y^{-1} is expected from a watershed that has a large fraction of its surface in a condition similar to a construction site.

Table 3.2. Sediment yield from watersheds in California compared with yield from LLCW.					
Location	Watershed area km^2	Rainfall mm yr^{-1}	Sediment Yield tons km^{-2} yr^{-1}	Land cover	Reference
Southern CA	118 - 10,760	250-650	20-4200	Mixed natural, ag., urban	Inman and Jenkins 1999
Transverse Range, CA	9 - 1,000	397-877	600-2500[a]	Natural, some habitation	Scott, 1968
Transverse Range, CA	14 - 4,185	400-700	740-5300	Natural vegetation	Warrick and Mertes, 2009
Southern CA	288	330	500	Urban	Trimble 1997
Los Laureles Canyon	**11.6**	**100-330**	**4499-5040**	**Urban**	**This study**

a. Reported in m^3 km^{-2}, converted using 1.67 tons m^{-3}

4. CONCLUSION

The data collected allowed us to perform a comprehensive assessment of rainfall, runoff, and sediment load in the LLCW on the US-Mexico border. The observations suggest that:

1. Rainfall intensity is a critical control on event peak discharge, and event rainfall-runoff relationships are consistent with a SCS CN that is consistent with a partially urbanized watershed (CN 80-90).

2. Event-mean suspended sediment concentration (SSC) was relatively stable for a wide range of discharge, up to a maximum of 27 g/L. The slope of the Q-SSC relationship is low, indicating that sediment in the watershed is highly mobile sediment and is transported at a wide range of flows.

3. Annual total sediment load observed in sediment traps at the outlet correlates linearly with annual total rainfall. This is somewhat unexpected given the non-linear relationship between rainfall and runoff, and given previous observations in semi-arid regions (Inman and Jenkins, 1999), and may be due to overestimation of the trap efficiency for higher annual loads.

4. Annual sediment yield is higher than in most other watersheds in California, and is consistent with extremely high rates of erosion.

Future work will quantify the roles of different erosion processes in the sediment budget, and will model the production of sediment under different land cover and management scenarios.

5. REFERENCES

AMEC Earth & Environmental Inc. (2007). *Goat Canyon Retention Basin Soil Particle Size Distribution Study*. San Diego, CA.

Asselman, N. E. M. (2000). Fitting and interpretation of sediment rating curves. Journal of Hydrology, 234(3–4), 228–248. doi.org/10.1016/S0022-1694(00)00253-5.

Biggs, T. W., Atkinson, E., Powell, R., & Ojeda-Revah, L. (2010). Land cover following rapid urbanization on the US–Mexico border: Implications for conceptual models of urban watershed processes. *Landscape and Urban Planning*, *96*(2), 78–87. doi.org/10.1016/j.landurbplan.2010.02.005

Crawford, C. G. (1991). Estimation of suspended-sediment rating curves and mean suspended-sediment loads. Journal of Hydrology, 129(1–4), 331–348.

de Temple, B., Ruttenberg, D., Perala, N. C., & Battalio, R. (1999). *A preliminary design of a sediment retention facilities for Goat Canyon Creek*. Corte Madera, CA: Phil Williams and Associates, Ltd.

Dunne, T., & Leopold, L. B. (1978). Water in Environmental Planning. New York: W.H. Freeman and Company.

Grover, R., & Swanson, K. (2011). Local perspectives on environmental degradation and community infrastructure in Los Laureles Canyon, Tijuana, Mexico. Geography. San Diego State University, San Diego.

Inman, D. L., & Jenkins, S. A. (1999). Climate Change and the Episodicity of Sediment Flux of Small California Rivers. The Journal of Geology, 107, 251-270.

Morris, G.L. and Fan, J. (1998). *Reservoir Sedimentation Handbook: Design and Management of Dams, Reservoirs and Watersheds for Sustainable Us*e. New York: McGraw-Hill Companies, Inc.

NOAA (National Oceanic and Atmospheric Administration) (2017). Precipitation Frequency Data Server, url: http://hdsc.nws.noaa.gov/hdsc/pfds/, access date 2017-06-07.

Rubey, W.R., 1933. *Settling velocities of gravel, sand and silt particles*. American Journal of Science, 21, 325-338.

Russell, K. L., Vietz, G. J., & Fletcher, T. D. (2017). Global sediment yields from urban and urbanizing watersheds. *Earth-Science Reviews*, *168*(Supplement C), 73–80. http://doi.org/https://doi.org/10.1016/j.earscirev.2017.04.001.

Soil Conservation Service. (1986). *Urban Hydrology for Small Watersheds, Technical Release 55*. Washington, D.C.

Southwest Wetlands Interpretive Association (SWIA) (2001). Final Environmental Impact Statement and Environmental Impact Report for the Goat Canyon Enhancement Project. Imperial Beach, CA.

Syvitski, J. P., Morehead, M. D., Bahr, D. B., & Mulder, T. (2000). Estimating fluvial sediment transport: the rating parameters. Water Resources Research, 36(9), 2747–2760.

Urbonas, B., and Stahre, P., (1993). *Stormwater Best Management Practices and Detention*. PTR Prentice Hall, Englewood Cliffs, New Jersey.

APPENDIX A. HYDROGRAPHS AND HYETOGRAPHS FOR ALL EVENTS

Table A1. Summary of storms and partitioning of rainfall into daily totals for analysis and modeling. The "*" indicates events that were not included in further analysis but were included for reallocation of rainfall. E1, E2 or E3 indicate the events retained for analysis. Observed and revised rainfall are from the Hormiguitas gage (RG.HM).

	Daily rainfall (mm)	Event total rainfall (mm)	Event start	Event end	Maximum Intensity (mm)			SCS Storm Type
Storm 1					15 min	1 hr	6 hr	
2/27/2014*	1.3	1.3	2014-02-27 07:40	2014-02-28 00:00	0.75	0.75	1	-
E1: 2/28/2014	19.7	12.2	2014-02-28 00:00	2014-02-28 15:50	2.75	5.75	9.75	12T2
E2: 3/1/2014	10.5	7.5	2014-02-28 15:50	2014-03-01 00:00	6.0	7.25	7.75	6T2
E3: 3/2/2014	0.5	7.5	2014-03-01 00:00	2014-03-01 15:57	3.25	6.0	7.25	-
3/3/2014*	0	3.5	2014-03-01 15:57	2014-03-02 12:13	1.5	1.5	3	-
Total	32.0	32.0						
Storm 2								
2015-02-28*	1.3	1.3	2015-02-28 11:26	2015-03-01 00:00	1.25	1.25	1.25	-
E1: 2015-03-01	29.5	23.3	2015-03-01 00:00	2015-03-01 22:19	1.75	5.75	16.0	24T1
E2: 2015-03-02	5.2	9.2	2015-03-01 22:19	2015-03-02 11:29	2.75	6.25	7.75	24T1
2015-03-03*	0.3	2.5	2015-03-02 11:30	2015-03-03 02:00	2.5	2.5	4.0	-
Total	36.3	36.3						
Storm 3								
2015-05-14*	1.5	1.5	2015-05-14 14:31	2015-05-15 00:00	0.5	0.5	1.75	-
E1: 2015-05-15	22.5	22.5	2015-05-15 00:00	2015-05-15 13:14	4.25	10.25	19	12T2
Total	24.0	24.0						
Storm 4								
E1: 2015-09-15	29.5	30.8	2015-09-15 10:47	2015-09-16 05:52	3.5	11.25	21	24T1
2015-09-16*	1.3	0	2015-09-16 05:52	--				-
Total	30.8	30.8						
Storm 5								
2016-01-04*	14.3	15	2016-01-04 02:27	2016-01-05 09:18	3	3.5	7	-
E1: 2016-01-05	23.0	22.3	2016-01-05 09:18	2016-01-05 18:33	4.75	8.5	20	12T2
2016-01-06*	5.5	5.5	2016-01-05 18:33	2016-01-06 20:08	2.5	2.5	4.25	-
2016-01-07*	6.5	6.5	2016-01-06 20:08	2016-01-07 23:56	0.5	2	3.5	-
2016-01-08*	1	1	2016-01-07 23:56	2016-01-08 04:28	1	1	1	-
Total	50.3	50.3						
Storm 6								
2016-03-05*	1.0	0	-	-				
E1: 2016-03-06	5.5	6.5	2016-03-05 20:44	2016-03-06 08:55	0.25	0.5	1.25	16T2

E2: 2016-03-07	23.0	23.0	2016-03-06 9:00	2016-03-08 10:07	4.75	8.5	16.25	12T2
2016-03-09*	0.2	0.2	2016-03-09 5:12	2016-03-11 15:55	0.25	0.25	0.25	-
2016-03-11*	3.8	3.8	2016-03-11 15:55	2016-03-11 17:36	1	2.25	3.75	-
Total	33.5	33.5						
Storm 7								
2016-04-07*	8.8	8.8	2016-04-07 6:37	2016-04-07 14:46	1.5	2.5	8	-
2016-04-08*	1.2	1.2	2016-04-07 14:50	2016-04-08 7:18	0.25	0.75	1	-
2016-04-09/10*	3.8	3.8	2016-04-09 19:44	2016-04-10 4:47	0.75	1.25	3.25	-
Total	13.8	13.8						
Storm 8								
2017-01-17/18*	1.2	0	--	--				
E1: 2017-01-19	11.8	13.0	2017-01-17 3:49	2017-01-19 12:00	2.75	6	11.75	6T2
E2: 2017-01-20	28.0	28.0	2017-01-20 2:30	2017-01-21 23:00	4	6	14.25	16T1
2017-01-22*	11.0	11.0	2017-01-22 17:50	2017-01-22 23:26	1	3.5	11	-
2017-01-23*	13.0	13.0	2017-01-23 3:05	2017-01-24 06:00	5.75	7	11	-
Total	65.0	65.0						
Storm 9								
E1: 2017-02-17	31.0	33.2	2017-02-17 17:50	2017-02-18 20:00	4.25	9.5	30.5	6T1
2017-02-18*	8.0	5.8	2017-02-18 20:00	2017-02-18 23:15	1.75	3	3	-
2017-02-19*	2.3	2.3	2017-02-19 2:59	2017-02-19 12:20	0.75	1	1.75	-
2017-02-22*	0.5	0.5	2017-02-22 1:18	2017-02-22 7:58	0.25	0.25	0.25	-
Total	41.8	41.8						
Storm 10								
2017-02-26*	2.0	0	--	--				
E1: 2017-02-27	74.5	83.0	2017-02-26 8:44	2017-02-28 13:28	1.75	6.25	33.25	24T1
2017-02-28*	6.5	0	--	--				-
Total	83.0	83.0						

Table A2. Summary of storm events defined in Table 2.3. Source refers to which gage was used as the final observed data.

Event Date*	Rainfall (mm)	Peak Discharge (cms)		Total Runoff (mm)		Runoff Ratio (Q/P)		Event	Source
		PT	IBWC	PT	IBWC	PT	IBWC		
Storm 1									
2014-02-28	12.25	1.13	0.05	0.27	0.02	0.02	0.00	E1	PT

2014-03-01	7.50	0.50	1.54	0.13	0.33	0.02	0.04	E2	IBWC
2014-03-02	7.50	0.77	6.14	0.26	1.08	0.03	0.14	E3	IBWC
Storm 2									
2015-03-01	23.25	3.36	-	1.36	-	0.06	-	E1	PT
2015-03-02	9.25	1.43	-	0.48	-	0.05	-	E2	PT
Storm 3									
2015-05-15	22.50	19.46	-	5.93	-	0.26	-	E1	PT
Storm 4									
2015-09-15	30.75	5.27	-	6.40	-	0.21	-	E1	PT
Storm 5									
2016-01-05	22.25	17.72	9.31	3.76	13.76	0.17	0.62	E1	PT
Storm 6									
2016-03-06	6.50	1.03	0.00	0.93	0.00	0.14	0.00	E1	PT
2016-03-07	23.00	1.78	5.07	1.81	4.23	0.08	0.18	E2	IBWC
Storm 8									
2017-01-19	13.00	-	5.37	-	2.57	-	0.20	E1	IBWC
2017-01-20	29.25	-	6.86	-	18.66	-	0.64	E2	IBWC
Storm 9									
2017-02-17	33.25	0.92	11.16	1.02	7.03	0.03	0.21	E1	IBWC
Storm 10									
2017-02-27	83.00	16.69	14.45	42.07	43.44	0.51	0.52	E1	CAMERA

No PT data for storm 7, IBWC rating curve discharge was zero.

Table A2 generated from: https://github.com/kristaniguchi/EPA_Events_Report_TJ_LLCW_Scripts/blob/master/Table2.2_2.3_EventsReport_generate.R (generate tables from each events script), https://github.com/kristaniguchi/EPA_Events_Report_TJ_LLCW_Scripts/blob/master/Table2.2_EventsReport_html_format.R (format as html table)

Storm 2: 2015-03-01 to 2015-03-03

This storm had three distinct storm hydrographs (Figure A1). We separated them into two storms, one for 2015-03-01 and one for 2015-03-02 (Table 2.3). The third event was small and was excluded from the model calibration and validation. The rainfall was closest to a 24-hour, Type I storm (Figure A2).

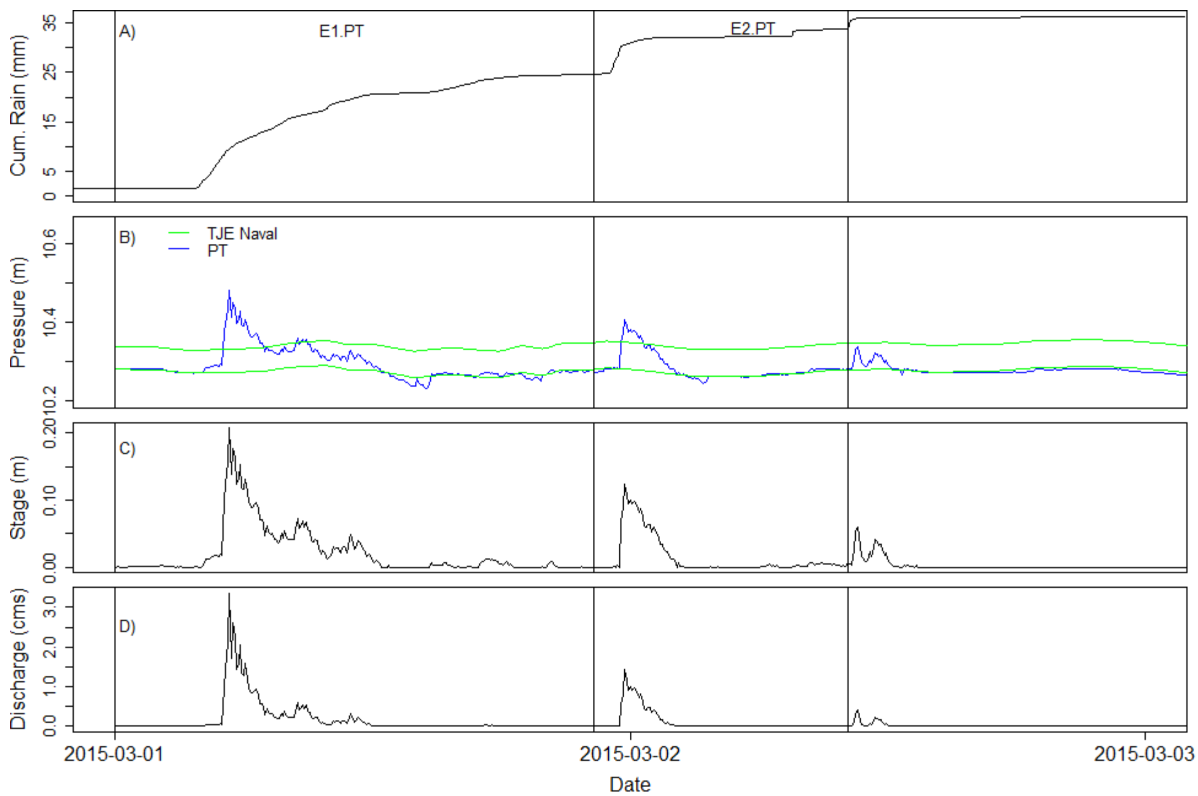

Figure A1. Storm 2, 2015-03-01 to 2015-03-03, with A) cumulative rainfall, B) pressure, including atmospheric pressure from the weather stations (upper green line), adjusted atmospheric pressure (lower green line), and pressure from the PT (blue), C) water stage, and D) discharge. The vertical dashed lines indicate where events were defined to start and end for purposes of reallocating rainfall and runoff data (Table 2.3). E1.PT and E2.PT indicate the two events that were retained for analysis. https://github.com/kristaniguchi/EPA_Events_Report_TJ_LLCW_Scripts/blob/master/figure_2.07_storm2_PT_2015_03_01_KTedits04202017.R

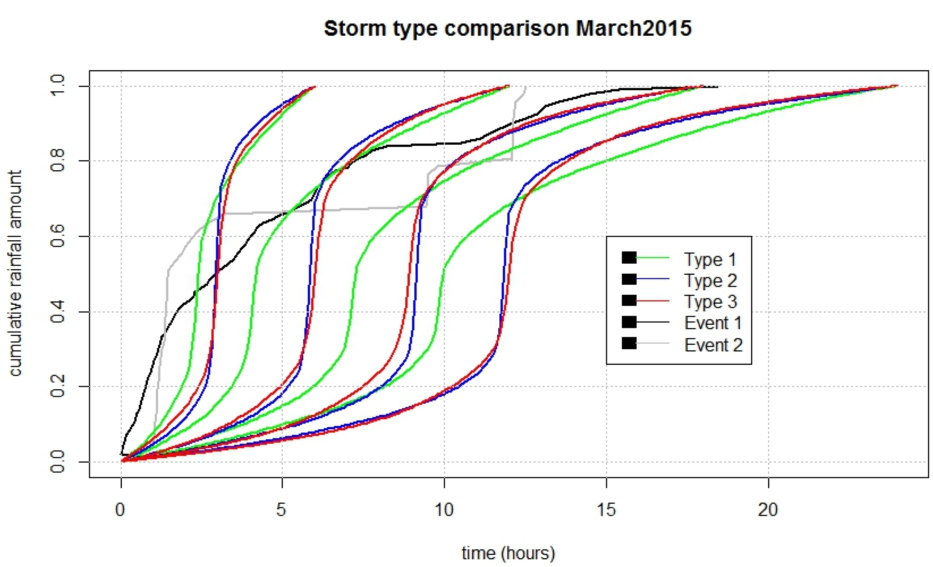

Figure A2. Cumulative rainfall amount, normalized to event total rainfall, for the two events in March 2015 (Storm 2).

Storm 3: 2015-05-15

This storm had one hydrograph event that occurred in the middle of the day, and the observed rainfall and runoff time series were not changed for model input (Figure A3). This storm was an outlier for peak discharge. The storm has higher maximum intensity than the Type II storm (Figure A4).

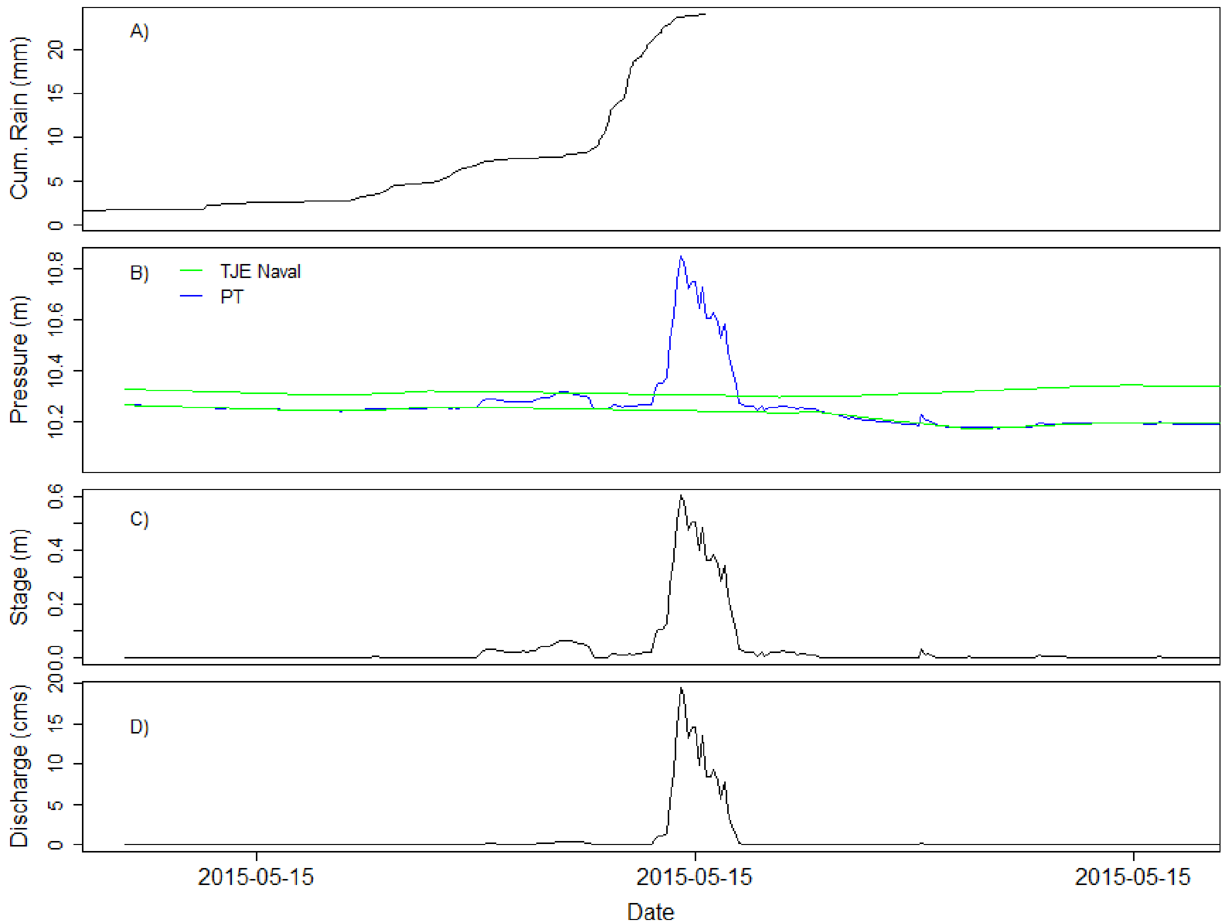

Figure A3. Storm event #3, 2015-05-15, with A) cumulative rainfall, B) pressure, including atmospheric pressure from the weather station (upper green line), adjusted atmospheric pressure (lower green line), and pressure from the PT (blue), C) water stage, and D) discharge. One event was used for model validation, on 5/15/2015. Prepared with https://github.com/kristaniguchi/EPA_Events_Report_TJ_LLCW_Scripts/blob/master/figure_2.09_storm3_PT_2015_05_15_KTedits04202017.R

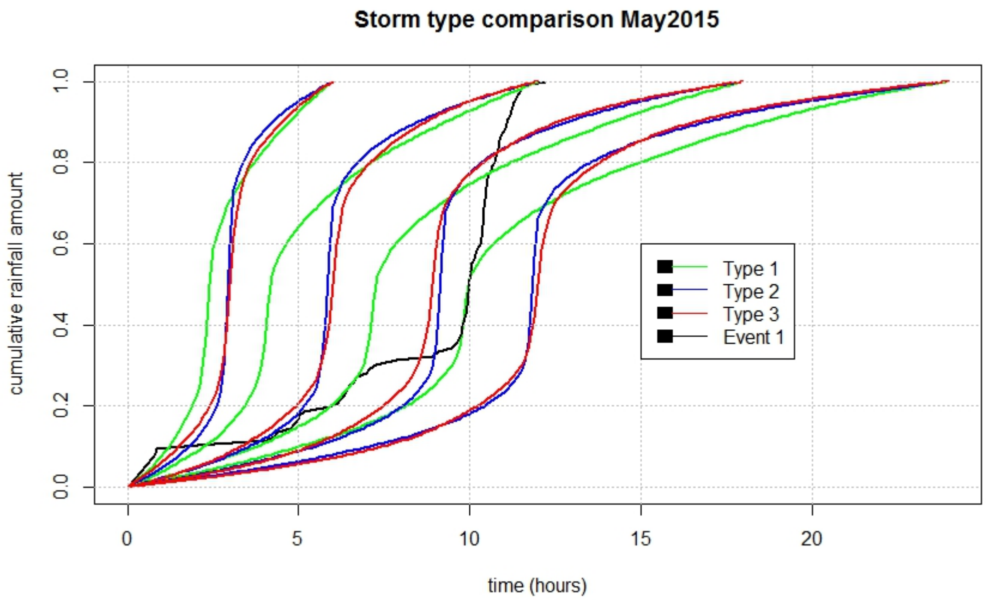

Figure A4. Cumulative rainfall amount, normalized to storm total rainfall, for the one event in May 15, 2015. This storm was an outlier for peak discharge.

Storm 4: 2015-09-15

This storm has one hydrograph event (Figure A5). The event occurred on 2015-09-15 and was not changed from the observed rainfall and runoff time series. A second event, on 2015-09-16, occurred after rainfall stopped and is not shown. The reason for the second peak is not known but is likely due to precipitation in the watershed not captured by the rain gages. Subsequent tests of the PT suggest that the instrument deployed during this storm shows spontaneous fluctuation, and was replaced for subsequent events. The rainfall was 24-hour type I (Figure A6).

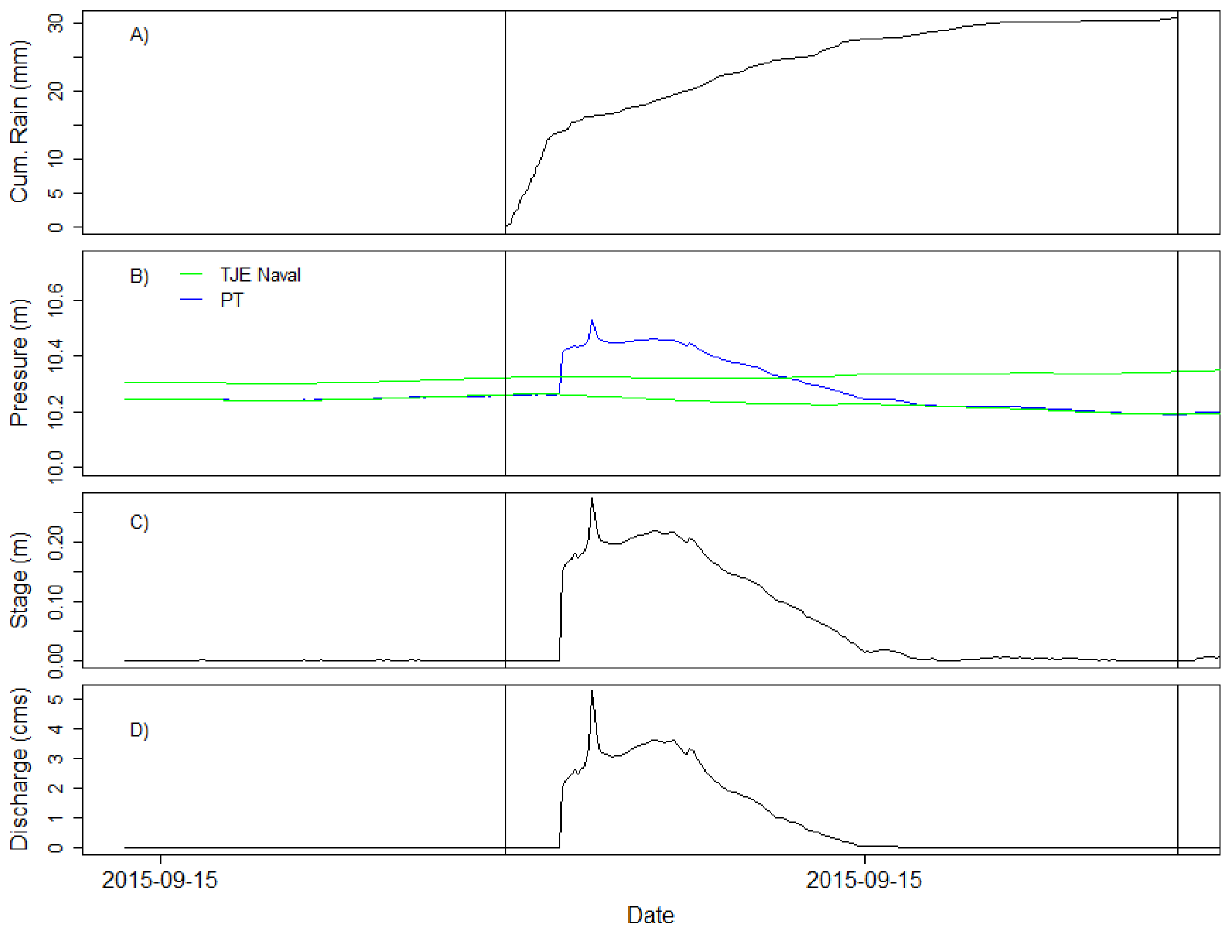

Figure A5. Storm event #4, 2015-09-15, with A) cumulative rainfall, B) pressure, including atmospheric pressure from the weather station (upper green line), adjusted atmospheric pressure (lower green line), and pressure from the PT (blue), C) water stage, and D) discharge. Vertical lines indicate the start and end of the one event retained for model validation. Prepared with https://github.com/kristaniguchi/EPA_Events_Report_TJ_LLCW_Scripts/blob/master/figure_2.11_storm4_PT_2015_09_15_KTedits04202017.R

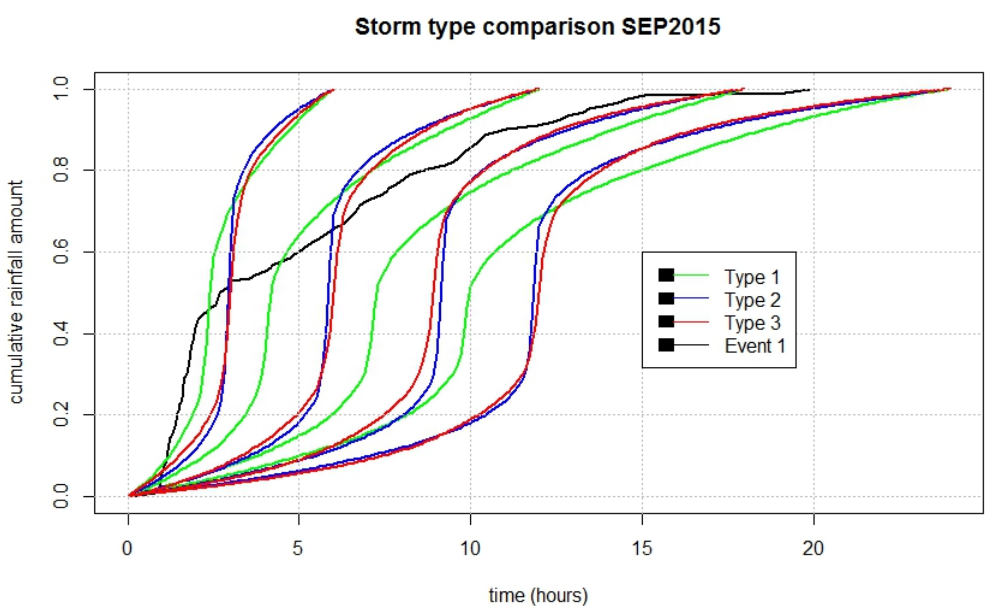

Figure A6. Cumulative rainfall amount, normalized to storm total rainfall, for the one event in September, 2015. 24-hour type I.

Storm 5: 2016-01-05

This storm has one hydrograph event on 2016-01-05 (Figure A7), so no reallocation of rainfall or runoff data were performed. The rainfall most closely matched the 12-hour Type II storm (Figure A8).

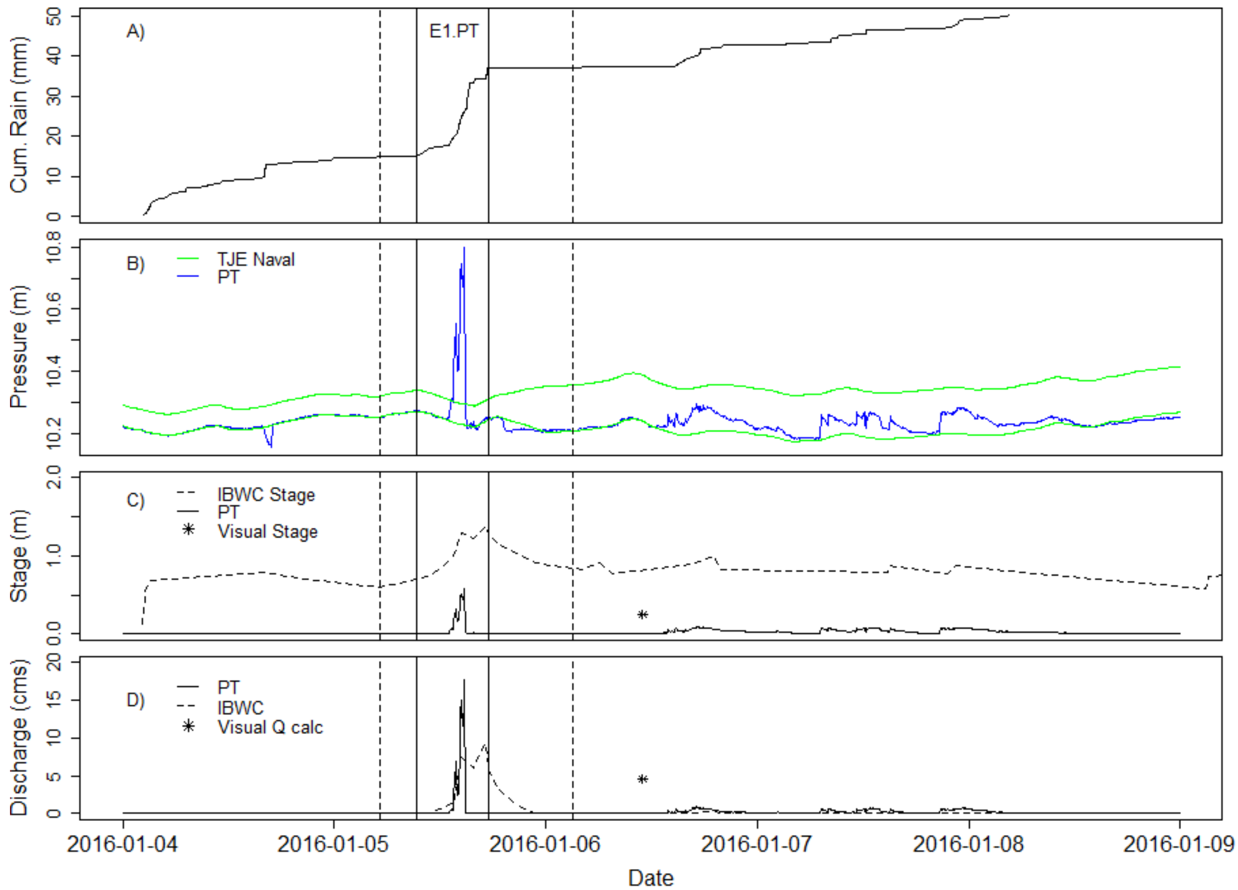

Figure A7. Storm event #5, 2016-01-05, with A) cumulative rainfall, B) pressure, including atmospheric pressure from the weather station (upper green line), adjusted atmospheric pressure (lower green line), and pressure from the PT (blue), C) water stage, and D) discharge. Vertical dashed lines indicate the start and end of the one event using IBWC BUBL stage. The vertical solid lines indicate the start and end of one event using the PT and was retained for model validation. Prepared with https://github.com/kristaniguchi/EPA_Events_Report_TJ_LLCW_Scripts/blob/master/figure_2.13_storm5_PT_2016_01_04_KTedits04172017.R

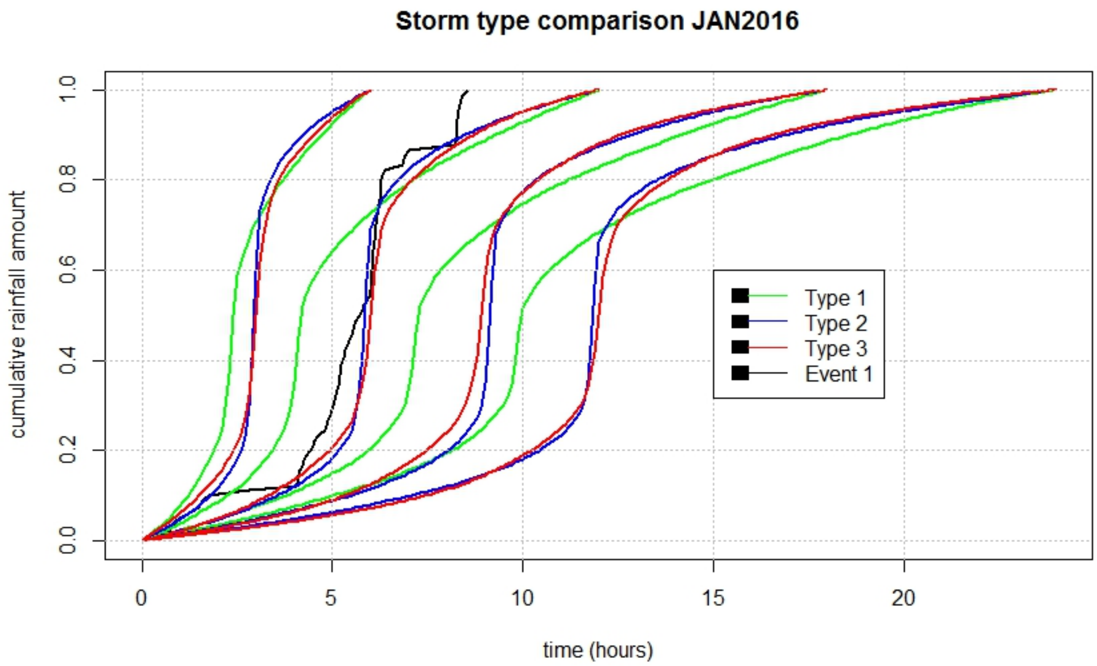

Figure A8. Cumulative rainfall for January, 2016. This storm was an outlier for peak discharge.

Storm 6: 2016-03-06

This storm has one hydrograph event on 2016-03-06 and one hydrograph event on 2016-03-07 to 2016-03-08 (Figure A9). The PT gave erratic measurements during the second event that did not correspond closely with rainfall, so the IBWC BBLR and ICBW-PT rating curve were used for that event. The rainfall did not match any storm type, but the peak intensity corresponded with a 16-hour, Type II storm (Figure A10).

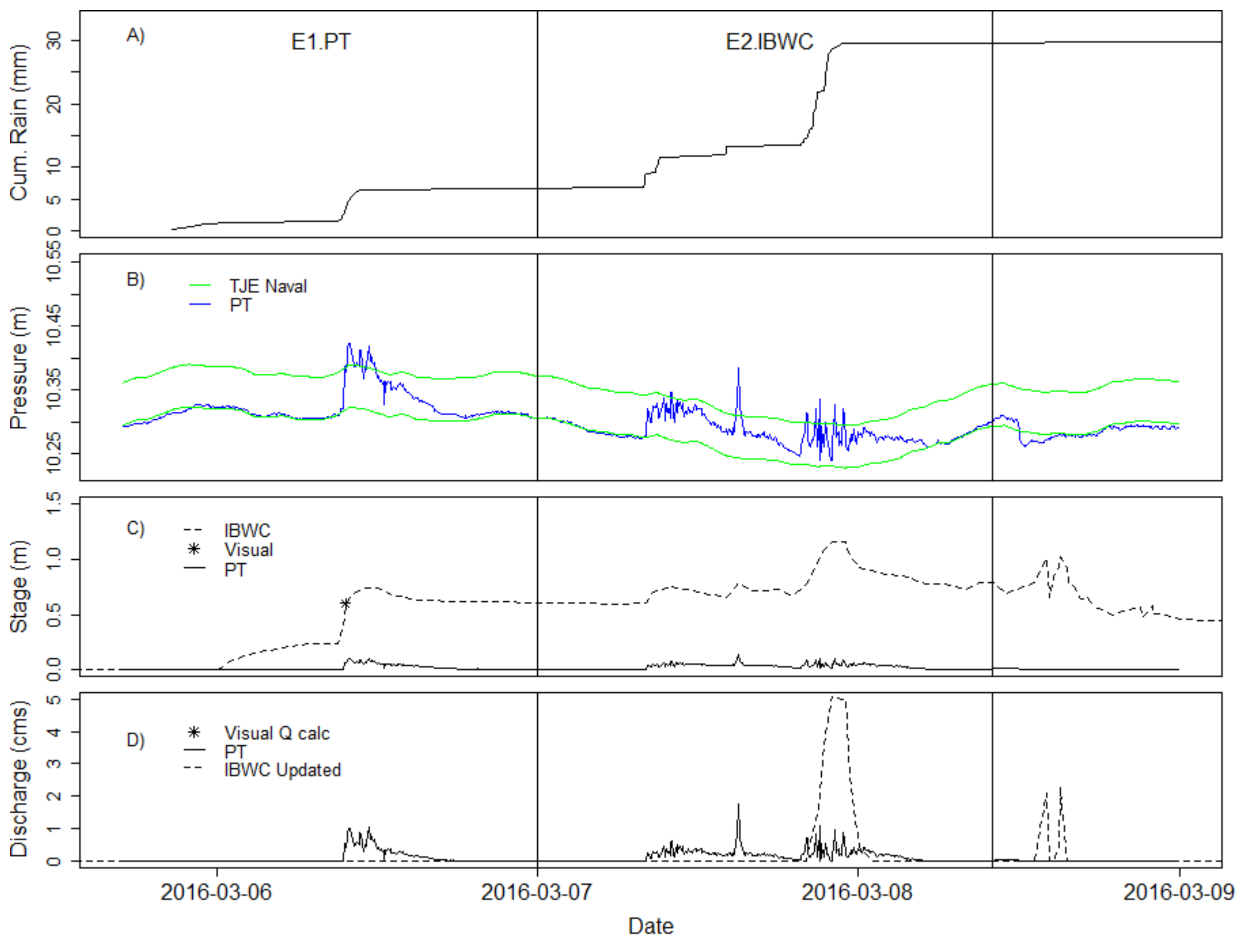

Figure A9. Storm event #6, 2016-03-06, with A) cumulative rainfall, B) pressure, including atmospheric pressure from the weather stations (upper green line), adjusted atmospheric pressure (lower green line), and pressure from the PT (blue), C) water stage, and D) discharge. Vertical lines indicate the start and end of the one event retained for model validation. The PT data for E2 were not used due to erratic measurements that do not correspond to the rainfall, so the IBWC BBLR data and IBWC-PT rating curve was used instead. Prepared with https://github.com/kristaniguchi/EPA_Events_Report_TJ_LLCW_Scripts/blob/master/figure_2.15_storm6_PT_2016_03b_KTedits04172017.R .

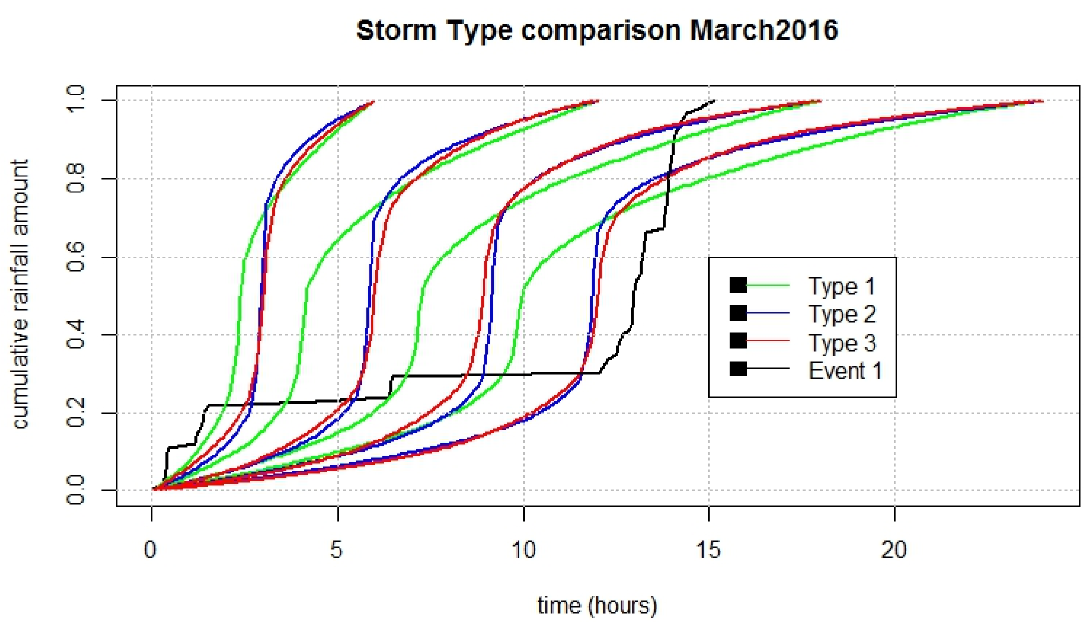

Figure A10. Cumulative rainfall for March, 2016.

Storm 7: 2016-04-09

This storm did not have recorded runoff at the PT, despite having significant rainfall (Figure A11). A malfunction of the PT must have occurred during this storm. Additionally, IBWC rating curve gave values of zero for this storm due to low stage measurements recorded from the bubbler. This storm was not included in subsequent analysis.

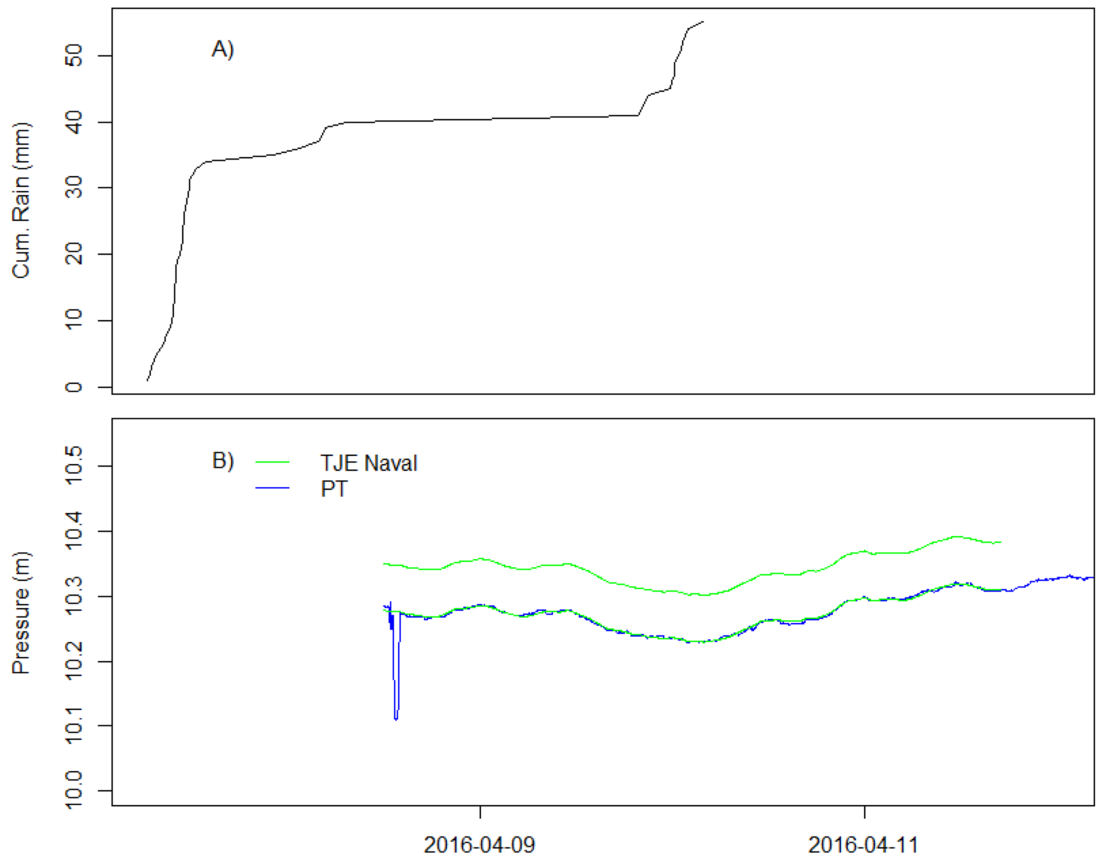

Figure A11. Storm event #7, 2016-04-09, with A) cumulative rainfall and B) pressure, including atmospheric pressure from the weather station (upper green line), adjusted atmospheric pressure (lower green line), and pressure from the PT (blue). No apparent discharge event captured with the PT, IBWC rating curve had discharge values of zero. Figure generated with https://github.com/kristaniguchi/EPA_Events_Report_TJ_LLCW_Scripts/blob/master/figure_2.17_storm7_PT_2016_04_KTedits04172017.R

Storm 8: 2017-01-19

A malfunction of the PT occurred during this storm. According to the IBWC rating curve, this storm had three major storm hydrograph (Figure A12). We retained two storms for analysis, one for 2017-01-19 and one for 2017-01-20 (Table 2.3). The third storm was erratic and didn't correspond well with rainfall and was excluded from the model calibration and validation. Storm was type 2, 6 hour (Figure A13).

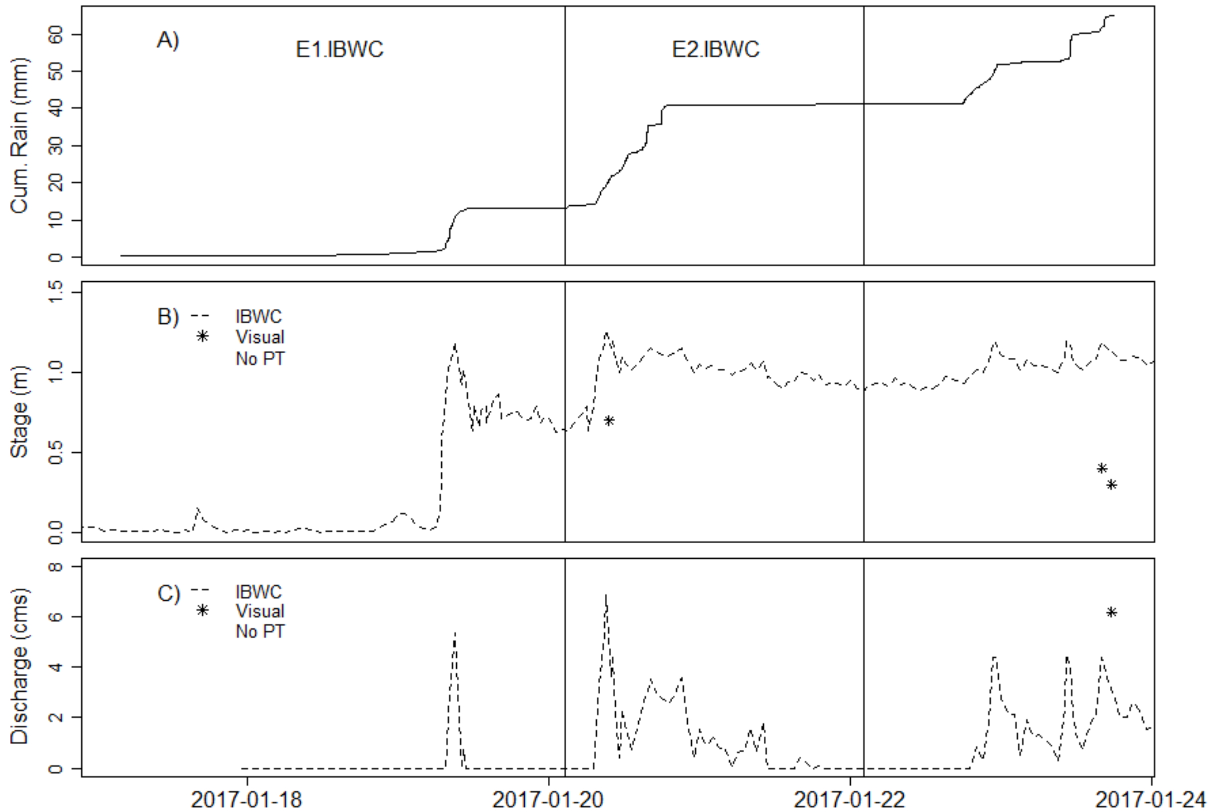

Figure A12. Storm event #8, 2017-01-18, with A) cumulative rainfall, B) stage from the IBWC bubbler, and C) discharge from the updated IBWC rating curve. No PT data were recorded, so the IBWC rating curve discharge were used. The "Visual" water levels and discharge are based on estimates at the PT location. Figure generated with https://github.com/kristaniguchi/EPA_Events_Report_TJ_LLCW_Scripts/blob/master/figure_2.18_storm8_IBWC_Visual_2017_01_KTedits04172017.R

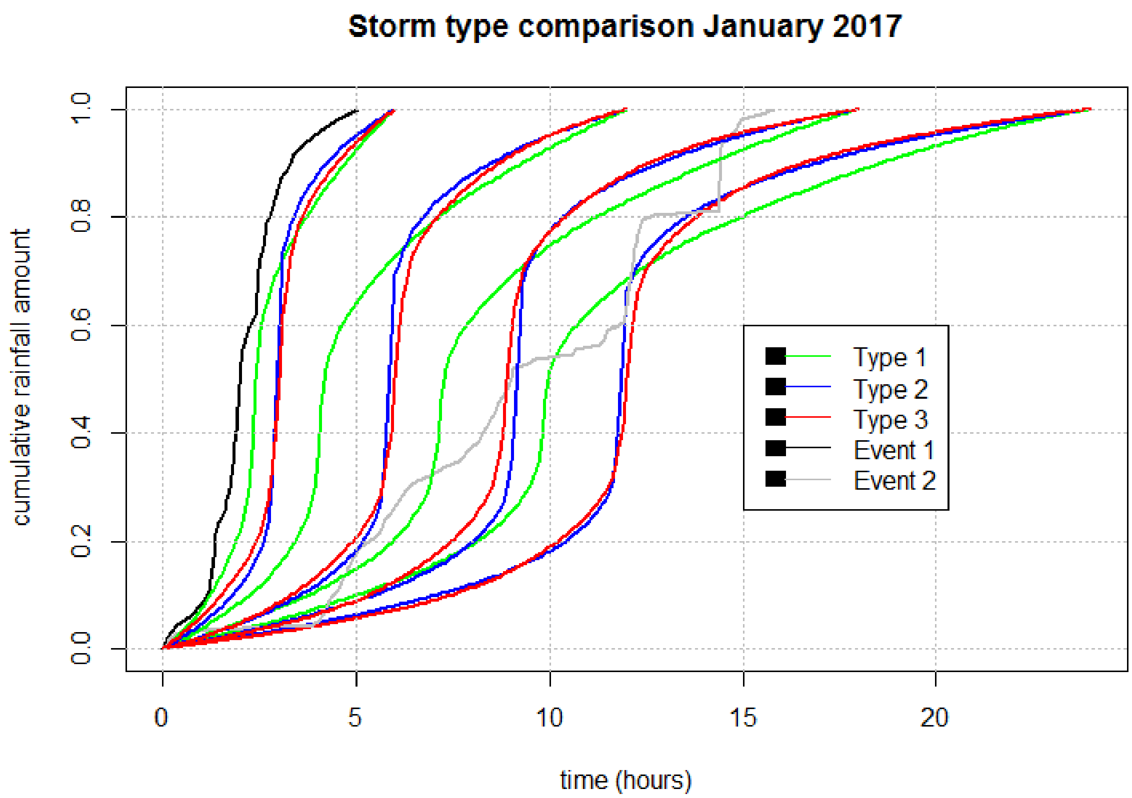

Figure A13. Cumulative rainfall for January 2017.

Storm 9: 2017-02-17

This storm had one distinct storm hydrograph (Figure A14). The PT housing was damaged during this storm and gave erratic measurements. Discharge calculated from the IBWC rating curve was used for the model calibration and validation. The IBWC peak discharge (~10 m^3 s^{-1}) matched well with the observed discharge (~15 m^3 s^{-1}). Storm was 6 hour type I (Figure A15).

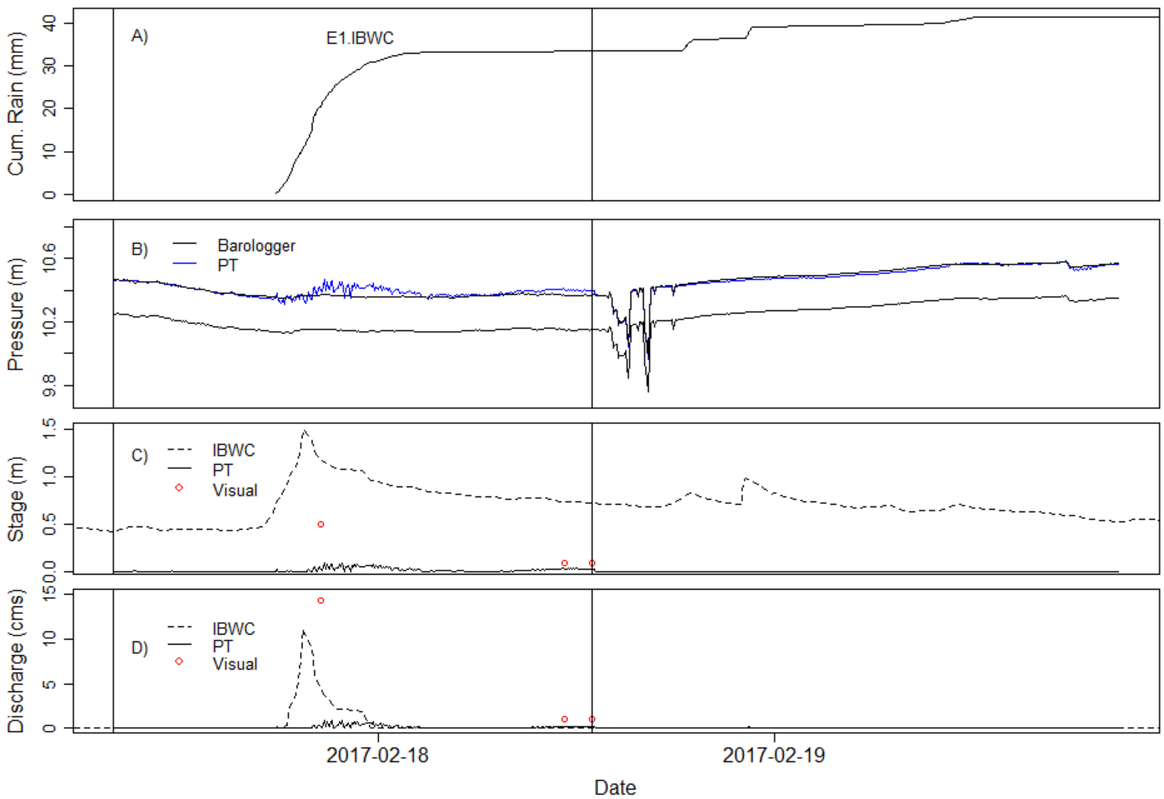

Figure A14. Storm event #9, 2017-02-17, with A) cumulative rainfall, B) pressure, including atmospheric pressure from the barologger (lower black line), adjusted atmospheric pressure (upper black line), and pressure from the PT (blue), C) water stage from the PT (solid black line) and IBWC bubbler (dashed black line), and D) discharge from the PT and IBWC rating curve. E1.IBWC indicates the one event was retained for the model and validation using the IBWC rating curve. Figure generated with https://github.com/kristaniguchi/EPA_Events_Report_TJ_LLCW_Scripts/blob/master/figure_2.19_storm9_IBWC_visual_2017_02_KTedits05012017.R

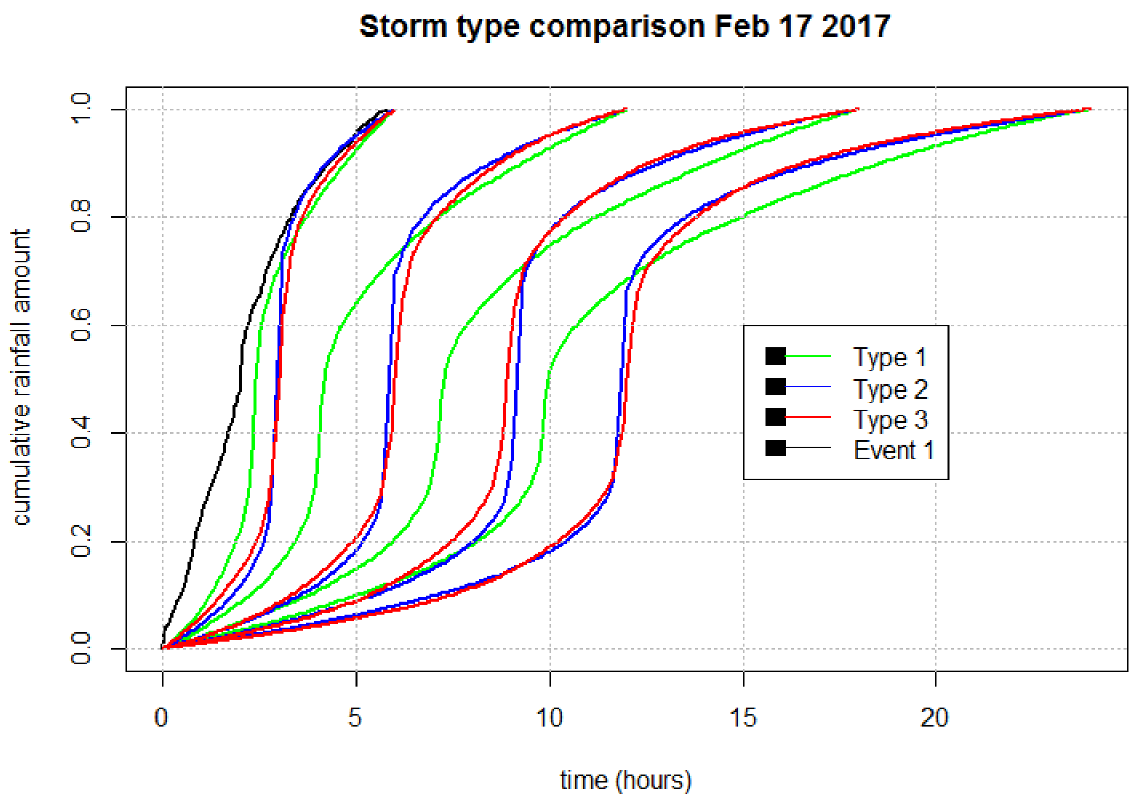

Figure A15. Cumulative rainfall for February 17, 2017.

Storm 10: 2017-02-27

This storm was the largest recorded observed storm and had one distinct storm hydrograph (Figure A16). There was no data from the PT, but a field camera was placed at the PT location and recorded stage every 15 minutes. The IBWC rating curve was developed from this event. Discharge calculated from the field camera was used for the model calibration and validation. Storm was 24h type I (A17).

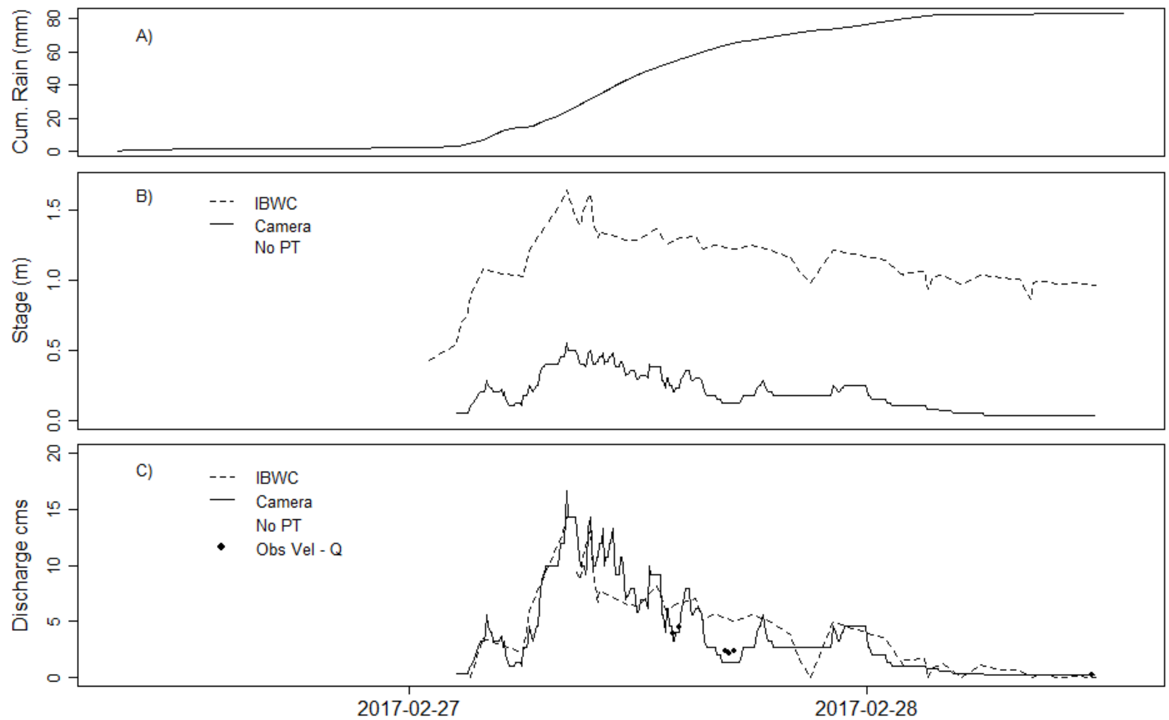

Figure A16. Storm event #10, 2017-02-27, with A) cumulative rainfall, B) stage recorded by the IBWC bubbler (dashed black line) and stage recorded by the field camera (solid black line), and C) discharge from the field camera and IBWC rating curve. IBWC rating curve was based on this event. Discharge from the field camera matched closely with observed discharge and was used in model calibration and validation. Figure generated with https://github.com/kristaniguchi/EPA_Events_Report_TJ_LLCW_Scripts/blob/master/figure_2.20_storm10_IBWC_visual_2017_0227_KTedits05012017.R

Figure A17. Cumulative rainfall for February 17, 2017.

APPENDIX B. HYDROGRAPHS DURING SSC MEASUREMENTS

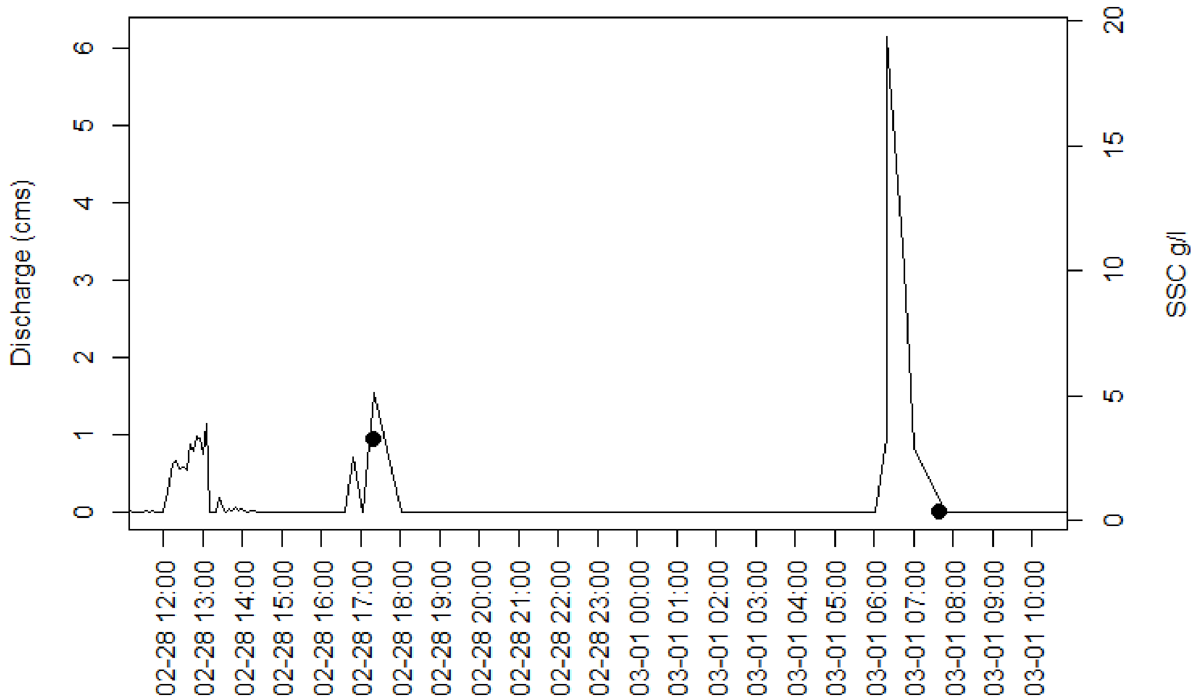

Figure B1. Hydrograph and SSC samples for 02/28/2014 - 03/01/2014. Figure generated from https://github.com/kristaniguchi/EPA_Events_Report_TJ_LLCW_Scripts/blob/master/Figure_3.2_EventsReport_SSC_03012014.R

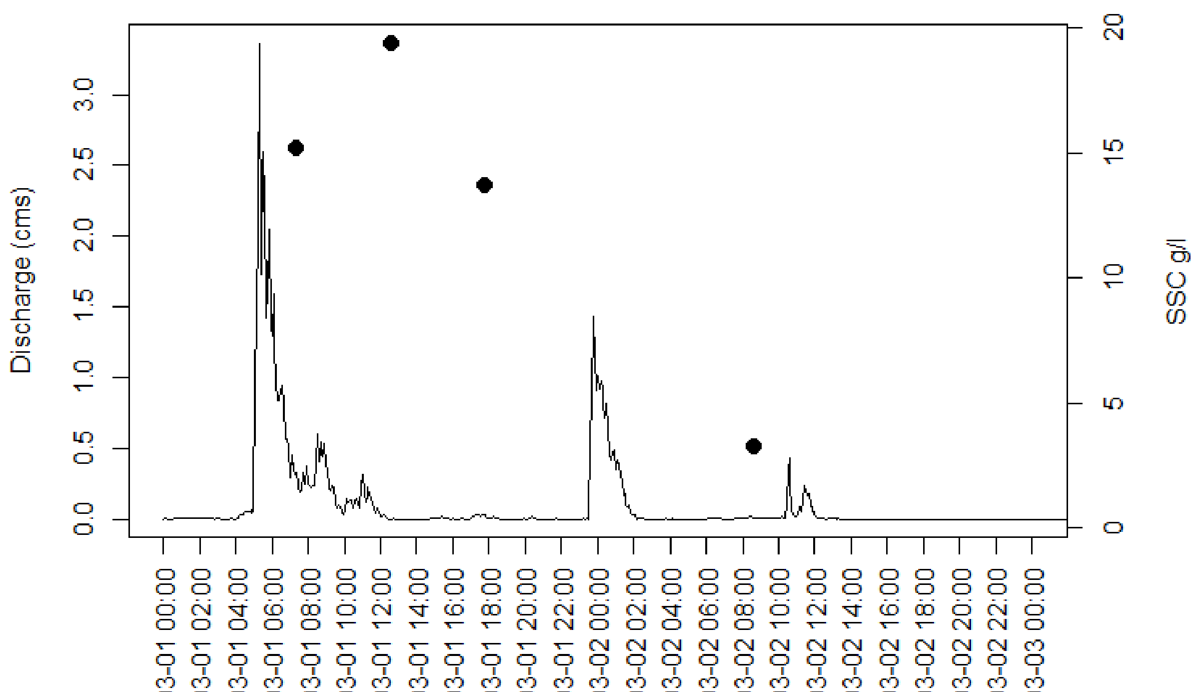

Figure B2. Hydrograph and SSC samples for Event on 2015-03-01. Figure generated from https://github.com/kristaniguchi/EPA_Events_Report_TJ_LLCW_Scripts/blob/master/Figure_3.3_EventsReport_SSC_030122015.R

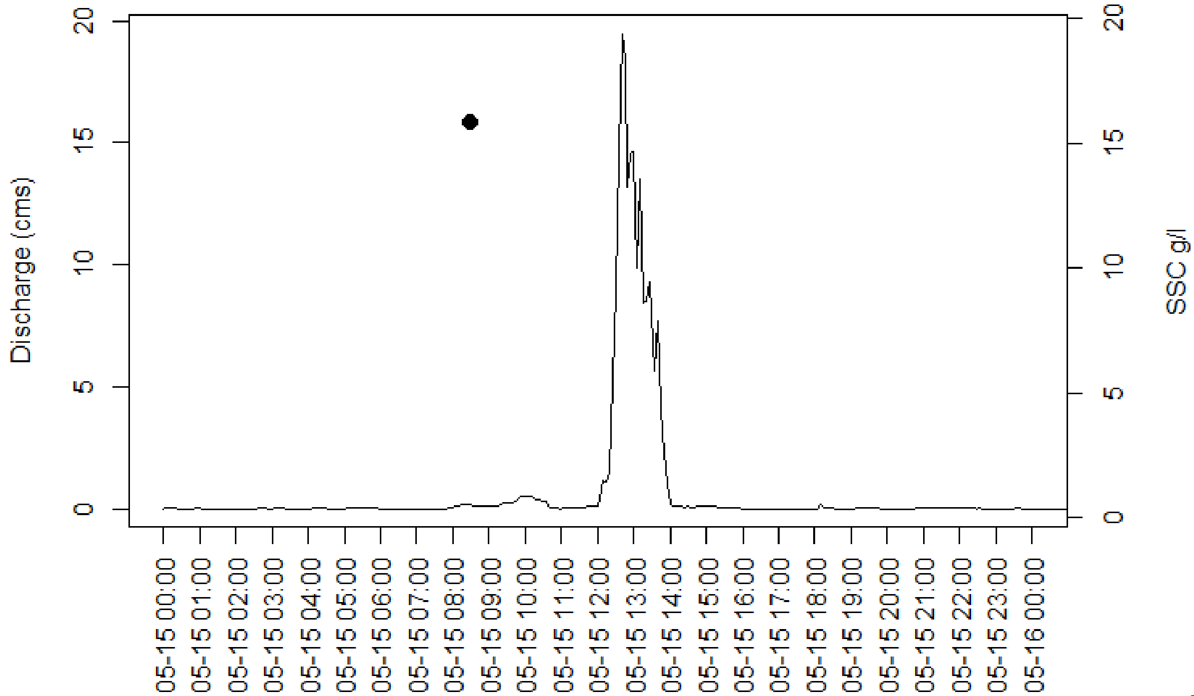

Figure B3. Hydrograph and SSC samples for 2015/05/15. Figure generated from https://github.com/kristaniguchi/EPA_Events_Report_TJ_LLCW_Scripts/blob/master/Figure_3.4_EventsReport_SSC_05152015.R

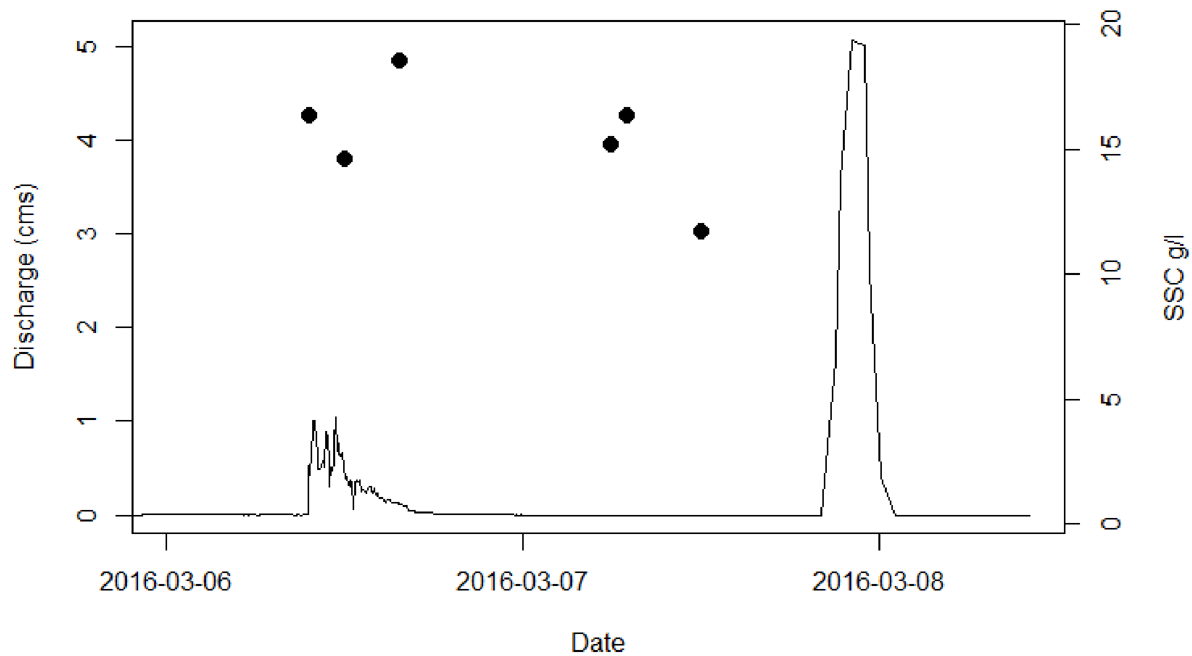

Figure B4. Storm 6: Hydrograph and SSC samples for 2016/03/6-8. Figure generated from https://github.com/kristaniguchi/EPA_Events_Report_TJ_LLCW_Scripts/blob/master/Figure_3.5_EventsReport_SSC_03062016.R

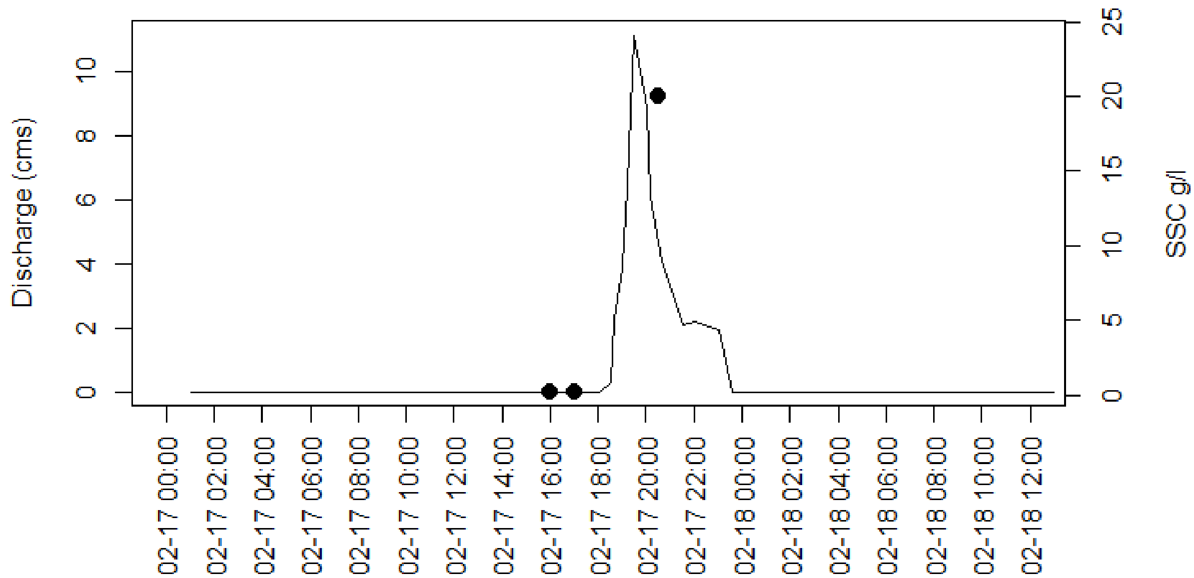

Figure B5. Storm 9: Hydrograph and SSC samples for 2017/02/17. Figure generated from https://github.com/kristaniguchi/EPA_Events_Report_TJ_LLCW_Scripts/blob/master/Figure_3.6_EventsReport_SSC_02172017.R

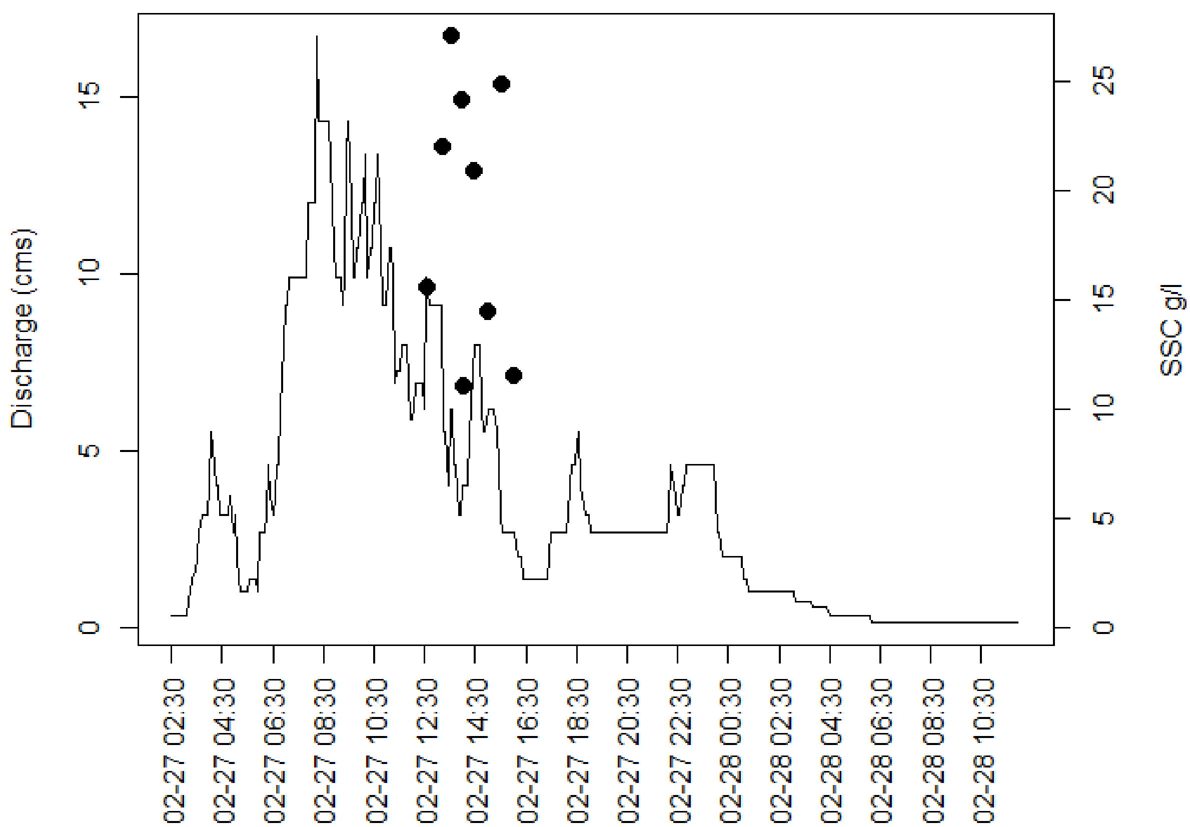

Figure B6. Storm 10: Hydrograph and SSC samples for 2017/02/27. Figure generated from https://github.com/tbiggsgithub/EPA_Events_Report_TJ_LLCW_Scripts/blob/master/Figure_3.7_EventsReport_SSC_02272017.R

APPENDIX C. SEDIMENT TRAP TEXTURE ANALYSES AND TRAP EFFICIENCY

Table C1. Particle size data summary for the Goat Canyon sediment traps. All sample depths were 0-3 ft, and mean grain size description was "fine sand" for all samples. Samples SS1 through GC8 are from AMEC (2007). Samples from "Avulsion Basin #1 to Canyon Basin #2 are from de Temple et al. (1999).

Sample location	Sample ID		Particle size distribution, percent							
		Median grain size mm	Gravel	Sand			Silt	Clay	Silt + Clay	Total Sand
				Coarse	Med.	Fine				
Sorted Pile	SS1	0.098	0	0	17.11	45.79	31.31	5.78	37.10	62.9
	SS2	0.101	0	0	20.07	44.32	30.91	4.71	35.61	64.39
	SS3	0.094	0	0	12.39	50.82	33.62	3.17	36.79	63.21
	Mean ± sd	0.098± 0.003	0	0	16.5±3.9	47±3.4	31.9±1.5	4.6±1.3	36.5±0.8	63.5±0.8
Native Pile	NS1	0.122	0	0	27.55	43.05	26.16	3.24	29.4	70.60
	NS2	0.146	0	0	30.01	43.93	22.81	3.25	26.05	73.95
	NS3	0.152	0	0	28.3	47.04	20.66	4	24.65	75.34
	Mean ± sd	140± 0.016	0	0	28.6±1.3	44.7± 2.1	23.2± 2.8	3.5± 0.4	26.7± 2.4	73.3± 2.4
Upper Catchbasin	GC1	0.090	0	0	7.60	53.97	33.69	4.74	38.43	61.57
	GC2	0.075	0	0	3.48	47.67	43.19	5.65	48.85	51.15
	GC3	0.085	0	0	3.95	54.83	36.4	4.82	41.22	58.78
	GC4	0.075	0	0	10.08	40.33	42.62	6.96	49.58	50.42
	GC5	0.069	0	0	5.39	41.06	47.57	5.98	53.54	46.45
	Mean ± sd	0.079± 0.008	0	0	6.1±2.7	47.6±6.9	40.7±5.6	5.6±0.9	46.3±6.3	53.7±6.3
Lower catchbasin	GC6	0.082	0	0	9.04	45.02	40.47	5.47	45.94	54.06
	GC7	0.094	0	0	3.38	61.31	30.79	4.53	35.32	64.68
	GC8	0.102	0	0	18.73	43.16	33.09	5.02	38.11	61.89
	Mean ± sd	0.092± 0.010	0	0	10.4 ± 7.8	49.8 ± 10	34.8 ± 5.1	5±0.5	39.8±5.5	60.2±5.5
Avulsion basin	#1	-	0	-	-	-	-	-	37.0	63.0
Avulsion basin	#2	-	0	-	-	-	-	-	13.1	89.6

Silt basin	-	-	0	-	-	-	-	-	39.8	60.2
Canyon basin	#1	-	5.8*	-	-	-	-	-	16.1	78.1
Canyon basin	#2	-	5.9*	-	-	-	-	-	3.4	90.7

*Coarser fractions underestimated due to sampling methods.

The settling velocity (ω) for each sediment size was estimated using the equations in the Reservoir Sedimentation Handbook referring to the Rubey (1933) equation:

$$\omega = \frac{[1636(\rho_s - \rho)d^3 + 9\mu^2]^{0.5} - 3\mu}{500d} \qquad \text{(C1)}$$

where ω = terminal fall velocity (m s^{-1}); ρ_s = sediment density (kg m^{-3}); ρ = density of water (kg m^{-3}), assumed to be 1000 kg m^{-3}; μ = dynamic viscosity of water (N•s m^{-2}), assumed to be 1.31×10^{-3} N•s/m^{-2}, and d = particle diameter (m).

The critical settling velocity (ω_c) of the sedimentation basin was calculated as:

$$\omega_c = Q/A \qquad \text{(C2)}$$

where ω_c = critical settling velocity (m/s), which is the velocity of the slowest particle of the basin that will be 100% removed (Morris and Fan, 1998); Q = design discharge or inflow

(m^3 s^{-1}), and A = surface area of the sediment basin (m^2).

Table C2. Sediment removed from traps (Tons Removed), annual trap efficiency, and corrected sediment load from the watershed by size class.

Removal Date	Tons Removed	Eann n=1	Eann n=3	Corrected Load (tons)
2006				
Medium sand (a)	1947	1.00	1.00	1947
Fine sand (b)	15194	1.00	1.00	15194
Silt (c)	12991	0.99	1.00	12992
Clay (d)	1788	0.36	0.40	4508
Total	31920			34642
Total without Clay	30132			30133
2007				
Medium sand (a)	1947	1.00	1.00	1947
Fine sand (b)	15194	1.00	1.00	15194
Silt (c)	12991	0.99	1.00	12992
Clay (d)	1788	0.53	0.61	2946
Total	31920			33079
Total without Clay	30132			30133
2008				
Medium sand (a)	3115	1.00	1.00	3115
Fine sand (b)	24310	1.00	1.00	24310
Silt (c)	20786	0.96	1.00	20815
Clay (d)	2860	0.16	0.18	16339
Total	51072			64580
Total without Clay	48212			48241
2009				
Medium sand (a)	3536	1.00	1.00	3536
Fine sand (b)	27592	1.00	1.00	27592
Silt (c)	23593	0.95	1.00	23673
Clay (d)	3246	0.22	0.23	14148
Total	57967			68949
Total without Clay	54721			54801
2010				
Medium sand (a)	4284	1.00	1.00	4284
Fine sand (b)	33427	1.00	1.00	33427
Silt (c)	28581	0.97	1.00	28609
Clay (d)	3933	0.29	0.31	12615
Total	70224			78935
Total without Clay	66291			66320
2011				
Medium sand (a)	3951	1.00	1.00	3951
Fine sand (b)	30833	1.00	1.00	30833
Silt (c)	26364	0.93	0.99	26764

Clay (d)	3627	0.34	0.39	9416
Total	64776			70965
Total without Clay	61149			61549
2012				
Medium sand (a)	3505	1.00	1.00	3505
Fine sand (b)	27349	1.00	1.00	27349
Silt (c)	23385	0.99	1.00	23388
Clay (d)	3218	0.67	0.75	4271
Total	57456			58513
Total without Clay	54238			54242

Source: https://github.com/kristaniguchi/EPA_Events_Report_TJ_LLCW_Scripts/blob/master/Table4.2_trap_efficiency.R

a. 6.1% Medium sand: 0.25 – 0.5 mm (mean = 0.375 mm)
b. 47.6% Fine sand: 0.125 - 0.250 mm (mean = 0.1875 mm)
c. 40.7% Silt: 0.0039 - 0.0625 mm (mean = 0.0332 mm)
d. 5.6% Clay: 0.00098 - 0.0039 mm or <3.9 um (mean = 0.00244 mm)

The mean grain size diameter was used to calculate the trap efficiency for each size class.

Original data figures and reports from AMEC (2007)

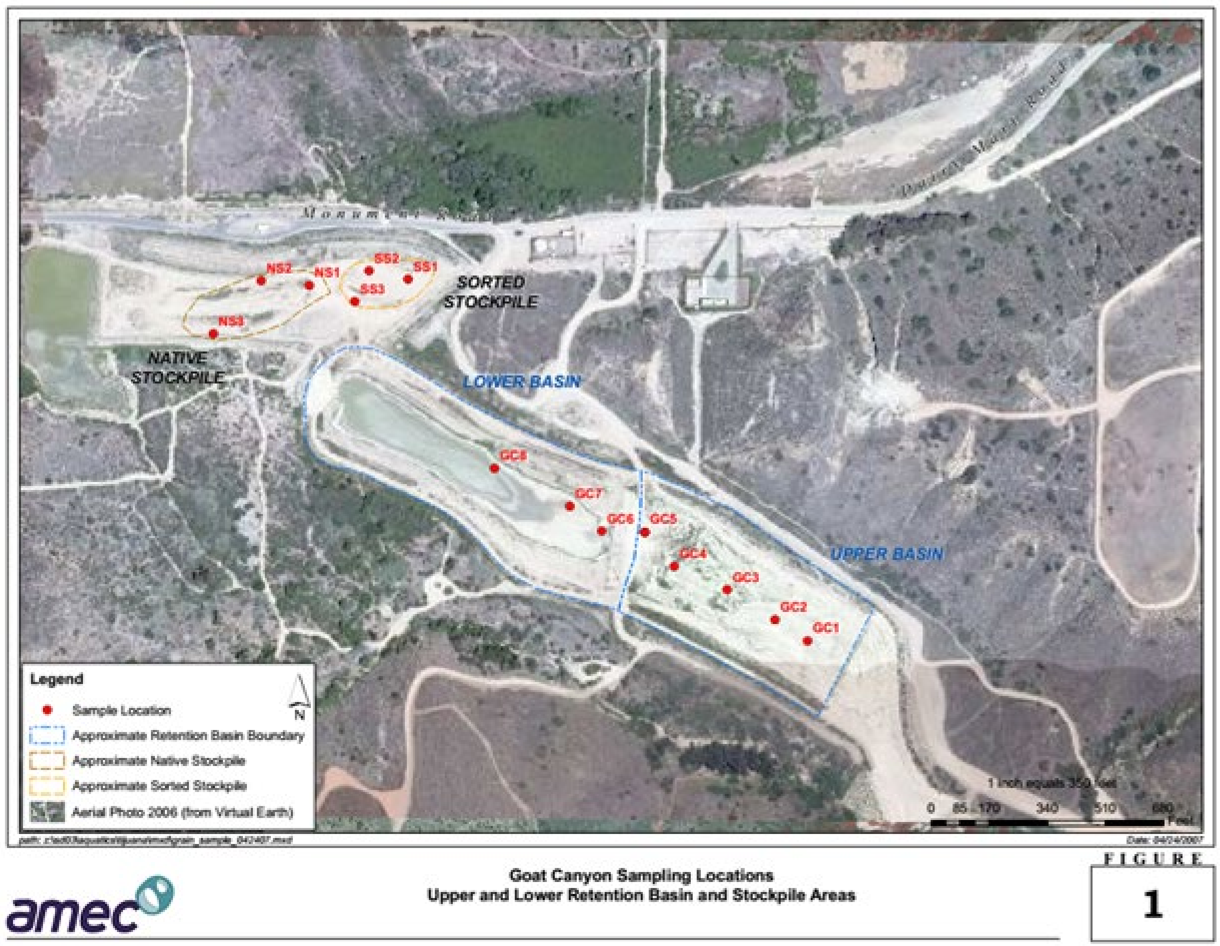

Figure C1. Sites analyzed for particle size by AMEC (2007).

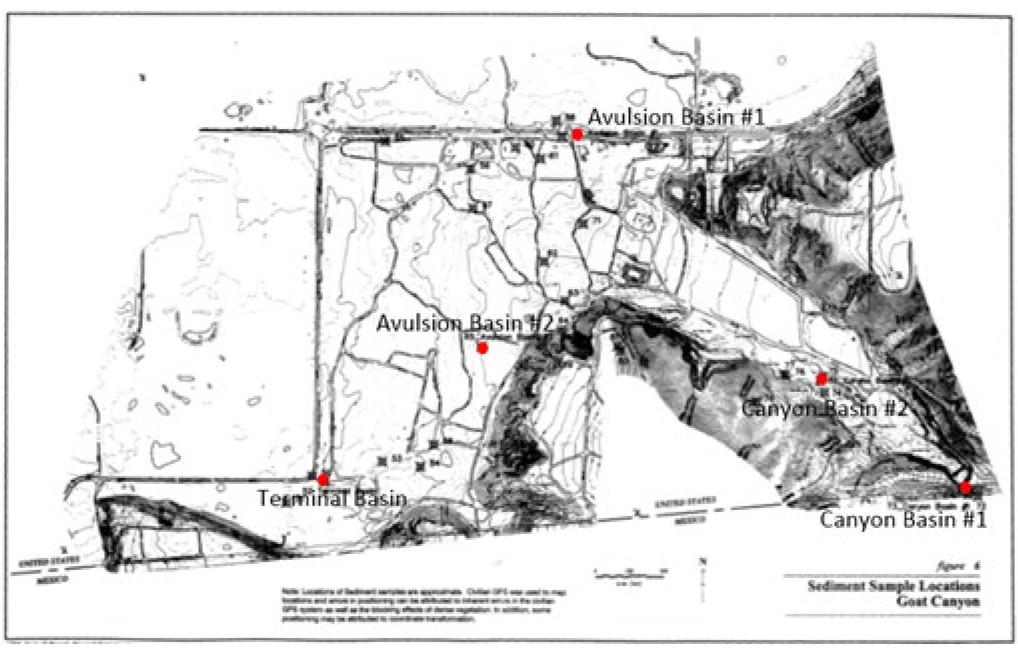

Figure C2. Sites analyzed for particle size by DeTemple et al. (1999). Sites are not located in the current sediment traps, but were taken in the Tijuana Estuary prior to constructing the sediment traps.

Table C3. Mean soil particle size data from AMEC (2007).

Table 2. Summary of Mean Soil Particle Size Data

Soil Sampling Area	Number of Samples	Percent Sand[1] (Mean ± SD)	Percent Fines[2] (Mean ± SD)	Median Grain Size (mm) (Mean ± SD)
Upper Basin	5	53.7 ± 6.3	46.3 ± 6.3	0.079 ± 0.008
Lower Basin	3	60.2 ± 5.5	39.8 ± 5.5	0.092 ± 0.010
Native Stockpile	3	73.3 ± 2.4	26.7 ± 2.4	0.140 ± 0.016
Sorted Stockpile	3	63.5 ± 0.8	36.5 ± 0.8	0.098 ± 0.003

[1] - particle size range from 0.063 to 3.363 mm.
[2] - particle size below 0.063 mm.
mm - millimeters
SD - standard deviation

Table C4. Raw data of particle size in the Goat canyon sediment traps, used to calculate the means in Table C1 (from Table C-1 in AMEC 2007).

Sample Collection Location	Sample ID	Depth, ft.	Mean Grain Size Description	Median Grain Size mm	Particle Size Distribution, wt. percent						Silt & Clay	Mean Percent Sand
						Sand Size						
					Gravel	Coarse	Medium	Fine	Silt	Clay		
Sorted Pile	SS1	0-3	Fine sand	0.098	0.00	0.00	17.11	45.79	31.31	5.78	37.10	62.90
	SS2	0-3	Fine sand	0.101	0.00	0.00	20.07	44.32	30.91	4.71	35.61	64.39
	SS3	0-3	Fine sand	0.094	0.00	0.00	12.39	50.82	33.62	3.17	36.79	63.21
	Mean			0.098	0.0	0.0	16.5	47.0	31.9	4.6	36.5	63.50
	Standard Deviation			0.003	0.0	0.0	3.9	3.4	1.5	1.3	0.8	0.78
Statistical Signficance (Sorted vs Native)?				Yes			Yes	NS			Yes	
Native Pile (Unsorted)	NS1	0-3	Fine sand	0.122	0.00	0.00	27.55	43.05	26.16	3.24	29.40	70.60
	NS2	0-3	Fine sand	0.146	0.00	0.00	30.01	43.93	22.81	3.25	26.05	73.95
	NS3	0-3	Fine sand	0.152	0.00	0.00	28.30	47.04	20.66	4.00	24.66	75.34
	Mean			0.140	0.0	0.0	28.6	44.7	23.2	3.5	26.7	73.30
	Standard Deviation			0.016	0.0	0.0	1.3	2.1	2.8	0.4	2.4	2.43
Upper Catchbasin	GC1	0-3	Fine sand	0.090	0.00	0.00	7.60	53.97	33.69	4.74	38.43	61.57
	GC2	0-3	Fine sand	0.076	0.00	0.00	3.48	47.67	43.19	5.65	48.85	51.15
	GC3	0-3	Fine sand	0.085	0.00	0.00	3.95	54.83	36.40	4.82	41.22	58.78
	GC4	0-3	Fine sand	0.075	0.00	0.00	10.08	40.33	42.62	6.96	49.58	50.42
	GC5	0-3	Fine sand	0.069	0.00	0.00	5.39	41.06	47.57	5.98	53.54	46.46
	Mean			0.079	0.0	0.0	6.1	47.6	40.7	5.6	46.3	53.67
	Standard Deviation			0.008	0.0	0.0	2.7	6.9	5.6	0.9	6.3	6.27
Statistical Signficance (Upper vs Lower Catchbasin)?				NS			NS	NS			NS	
Lower Catchbasin	GC6	0-3	Fine sand	0.082	0.00	0.00	9.04	45.02	40.47	5.47	45.94	54.06
	GC7	0-3	Fine sand	0.094	0.00	0.00	3.38	61.31	30.79	4.53	35.32	64.68
	GC8	0-3	Fine sand	0.102	0.00	0.00	18.73	43.16	33.09	5.02	38.11	61.89
	Mean			0.092	0.0	0.0	10.4	49.8	34.8	5.0	39.8	60.21
	Standard Deviation			0.010	0.0	0.0	7.8	10.0	5.1	0.5	5.5	5.51
Catchbasin Samples (Pooled)	Mean			0.084	0.000	0.000	7.706	48.420	38.478	5.396	43.874	49.89
	Standard Deviation			0.011	0.000	0.000	5.141	7.533	5.872	0.803	6.528	6.53

Figure C3. Photograph of sedimentation basin installed in winter 2013-14, Photo was taken on January 15, 2016.

Figure C4. Sediment sample taken at the retention basin on January 15, 2016.

APPENDIX D. LINKS TO DATA AND SCRIPTS

Figure 1.1 source code:
https://github.com/kristaniguchi/EPA_Events_Report_TJ_LLCW_ArcMap/blob/master/Figure_1.1_events_report_wtshd_map.mpk

Figure 2.1 Source code
https://github.com/kristaniguchi/EPA_Events_Report_TJ_LLCW_Scripts/blob/master/figure_1.2_hypsometric_dem_100bins.R

Elevation bins generated using:
https://github.com/kristaniguchi/EPA_Events_Report_TJ_LLCW_ArcMap/blob/master/Figure_1.2_hypsometric_curve_dem_clip_wtshd_forRscript.mpk

Figure 2.2 Source code:
https://github.com/tbiggsgithub/EPA_Events_Report_TJ_LLCW_Scripts/blob/master/precip_data_QC.R

Figure 2.3 Source code:
https://github.com/tbiggsgithub/EPA_Events_Report_TJ_LLCW_Scripts/blob/master/precip_data_QC.R

Figure 2.4 Source code:
https://github.com/tbiggsgithub/EPA_Events_Report_TJ_LLCW_Scripts/blob/master/precip_sum_over_storm_events.R

Table 2.3 Source code:

https://github.com/kristaniguchi/EPA_Events_Report_TJ_LLCW_Scripts/blob/master/Table2.2_2.3_EventsReport_generate.R (generate tables from each events script),
https://github.com/kristaniguchi/EPA_Events_Report_TJ_LLCW_Scripts/blob/master/Table2.2_EventsReport_html_format.R (format as html table)

Figure 2.6 Source code:

https://github.com/kristaniguchi/EPA_Events_Report_TJ_LLCW_Scripts/blob/master/figure_2.02_storm1_PT_2014_03_01_KTedits04172017.R

Figure 2.7 Source code:

https://github.com/kristaniguchi/EPA_Events_Report_TJ_LLCW_Scripts/blob/master/figure_2.04_ibwc_ratingcurve.R

Figure 2.9 Source code:
https://github.com/tbiggsgithub/EPA_Events_Report_TJ_LLCW_Scripts/blob/master/figure_2.5_rainfall_runoff_SCS_CN.R

Figure 2.10 Source code:

https://github.com/tbiggsgithub/EPA_Events_Report_TJ_LLCW_Scripts/blob/master/figure_2.6_Pmax_vs_Qmax.R

Table 2.4 Source code:

https://github.com/kristaniguchi/EPA_Events_Report_TJ_LLCW_Scripts/blob/master/Table3.1_3.3_EventsReport_generate.R and https://github.com/kristaniguchi/EPA_Events_Report_TJ_LLCW_Scripts/blob/master/Table3.1_EventsReport_html_format.R

Table 2.5 source code:
https://github.com/tbiggsgithub/EPA_Events_Report_TJ_LLCW_Scripts/blob/master/Table3.2_EventsReport_html_format.R

Figure 2.11 Source code:
https://github.com/tbiggsgithub/EPA_Events_Report_TJ_LLCW_Scripts/blob/master/regression_models_SSC_vs_Q.R

Figure 2.12 Source code:

https://github.com/tbiggsgithub/EPA_Events_Report_TJ_LLCW_Scripts/blob/master/figure_4.1b_break_dates.R